

Correct implementation of polarization constants in wurtzite materials and impact on III-nitrides

Cyrus E. Dreyer,^{1,2} Anderson Janotti,^{1,*} Chris G. Van de Walle,¹ and David Vanderbilt²

¹*Materials Department, University of California, Santa Barbara, CA 93106-5050*

²*Department of Physics and Astronomy, Rutgers University, Piscataway, NJ 08845-0849*

(Dated: September 25, 2018)

Accurate values for polarization discontinuities between pyroelectric materials are critical for understanding and designing the electronic properties of heterostructures. For wurtzite materials, the zincblende structure has been used in the literature as a reference to determine the effective spontaneous polarization constants. We show that, because the zincblende structure has a nonzero formal polarization, this method results in a spurious contribution to the spontaneous polarization differences between materials. In addition, we address the correct choice of “improper” versus “proper” piezoelectric constants. For the technologically important III-nitride materials GaN, AlN, and InN, we determine polarization discontinuities using a consistent reference based on the layered hexagonal structure and the correct choice of piezoelectric constants, and discuss the results in light of available experimental data.

PACS numbers: 77.22.Ej, 73.40.Lq, 85.60.Bt

I. INTRODUCTION

Pyroelectric materials have emerged in a variety of electronic and optoelectronic applications. Because of the symmetry of their crystal structure these materials exhibit spontaneous (SP) and piezoelectric (PZ) dipole moments [1] which manifest themselves as electric fields in heterostructure layers and sheet charges at interfaces. In the technologically important III-nitrides, which have the wurtzite (WZ) structure (space group $P6_3mc$), polarization differences allow for strong carrier confinement and the formation of a two-dimensional electron gas (2DEG) with high density at AlGaN/GaN interfaces, exploited in high electron mobility transistors (HEMTs). The effect of polarization can also be detrimental, for example causing the quantum-confined Stark effect in quantum wells of light-emitting diodes (LEDs), which reduces radiative recombination rates and shifts the emission wavelength. For both HEMTs and LEDs, accurate values of the SP and PZ polarization constants are required for a fundamental understanding as well as for device design.

Since experimental determination of the separate SP and PZ contributions to the total polarization is very difficult, calculated values of SP and PZ polarization constants are widely used in simulations. The PZ polarization constants are, in principle, fairly straightforward to explicitly measure or calculate [2]. However, the reported values exhibit a considerable spread [3]. In addition, the difference between so-called “proper” and “improper” PZ constants [2, 4] is often overlooked, even though it can give rise to significant quantitative changes in the resulting polarization fields. This difference is one issue that is elucidated in the present paper.

The definition of SP polarization constants is even more subtle, and they are typically not amenable to explicit experimental determination, except in special cases [5]. The calculation of SP polarization requires the choice of a reference structure, which in the case of WZ semiconductors, has invariably been chosen to be zincblende (ZB) [6–8]. In this work we will show that though ZB as a reference structure is intuitively appealing, the SP polarization constants that result have been misinterpreted, introducing a source of error into the predicted values for bound sheet charge densities (and polarization fields). We also demonstrate that a proper choice of reference structure can eliminate these problems, and we provide revised values that can be directly inserted in current simulation tools.

While our theoretical considerations are general, we choose the nitride semiconductors because they provide a suitable example to illustrate the derivations, and because our findings have a significant impact on this materials system of high (and still increasing) technological importance. In Sec. II we review the underlying theory. In Sec. III we address the problems with choosing zincblende as a reference structure, and propose a solution. Sec. IV deals with piezoelectric contributions, specifically the issue of proper versus improper constants. In Sec. V we show that our findings have important consequences for nitride device structures and compare with previous implementations and with experiment. Section VI concludes the paper.

II. CALCULATING POLARIZATION CONSTANTS IN WURTZITE

For WZ films grown in the [0001] direction (*i.e.*, the $+c$ direction), the polarization component P_3 is given by the sum of the SP polarization at the wurtzite material’s own lattice parameters, P_{SP} , and the z component of the

* Current address: Materials Science and Engineering, University of Delaware, Newark, Delaware 19716-1501, USA

PZ polarization [1]. That is, for material m ,

$$P_3^m = P_{\text{SP}}^m + (\epsilon_1^m + \epsilon_2^m)e_{31}^m + \epsilon_3^m e_{33}^m, \quad (1)$$

where (in Voigt notation) ϵ_i ($i=1,2,3$) is the strain in the i direction and e_{3i} are the corresponding piezoelectric constants (specifically, the ‘‘improper’’ ones; see Section IV). Henceforth we drop the subscript ‘‘3’’ from P for simplicity; all unbolded quantities pertaining to wurtzite are assumed to be in the c direction.

The goal of this work is to derive the appropriate SP and PZ constants that allow Eq. (1) to be used in accurately determining polarization differences at interfaces between different WZ materials.

A. The modern theory of polarization

Direct calculation of the polarization constants in Eq. (1) by first-principles electronic-structure methods was enabled by the formulation of a rigorous theory of bulk polarization, known as the modern theory of polarization (MTP) [9, 10]. For a given structure λ , the MTP allows calculation of the so-called ‘‘formal’’ polarization [9]:

$$\begin{aligned} \mathbf{P}_f &= \mathbf{P}_{\text{ion}} + \mathbf{P}_{\text{el}} \\ &= \frac{e}{\Omega} \sum_s Z_s^{\text{ion}} \mathbf{R}_s^{(\lambda)} + \frac{ief}{8\pi^3} \sum_j^{\text{occ}} \int_{\text{BZ}} d\mathbf{k} \langle u_{j,\mathbf{k}}^{(\lambda)} | \nabla_{\mathbf{k}} | u_{j,\mathbf{k}}^{(\lambda)} \rangle, \end{aligned} \quad (2)$$

where Ω is the cell volume, Z_s^{ion} is the charge of the ion s and $\mathbf{R}_s^{(\lambda)}$ is its position in the λ structure, f is the spin degeneracy of the bands, the sum j runs over occupied bands, and $u_{j,\mathbf{k}}^{(\lambda)}$ are the cell periodic parts of the Bloch wave functions. In Eq. (2), \mathbf{P}_{el} is the Berry phase taken over the valence-band manifold [9, 10]. The formal polarization is defined only modulo the ‘‘quantum of polarization’’ $e\mathbf{R}/\Omega$, where \mathbf{R} is any lattice constant and e is the electron charge [9, 10].

In the MTP, only *differences* between formal polarizations of appropriate structures, $\lambda = 0$ and $\lambda = 1$, are well defined:

$$\Delta \mathbf{P} = \mathbf{P}_f^{(\lambda=1)} - \mathbf{P}_f^{(\lambda=0)}. \quad (3)$$

The choice of the ‘‘appropriate’’ structures $\lambda = 0$ and $\lambda = 1$ rests on one of two possible considerations to ensure that physical conclusions can be drawn from their formal polarization differences. First, if the two structures are connected by an adiabatic, gap-preserving deformation path [9, 10], then their difference in polarization [$\Delta \mathbf{P}$ in Eq. (3)] is given by the expression

$$\Delta \mathbf{P} = \int_0^1 d\lambda \frac{\partial \mathbf{P}}{\partial \lambda}, \quad (4)$$

and corresponds to the zero-field adiabatic displacement current. This quantity can, in principle, be determined

experimentally. An obvious application is the calculation of piezoelectric constants, which involves polarization differences between structures with slightly different lattice constants and/or internal structural parameters.

B. Interface theorem

The second consideration, as shown by Vanderbilt and King-Smith [11], is that *if* an insulating interface can be constructed between two structures, the difference in formal polarization gives the bound charge, σ_b , that builds up at the interface as a result of the continuity of the displacement field over an interface with no free charge:

$$\sigma_b = (\mathbf{P}_f^{\lambda=1} - \mathbf{P}_f^{\lambda=0}) \cdot \hat{\mathbf{n}}. \quad (5)$$

This is often referred to as the ‘‘interface theorem.’’ Since there is no adiabatic path necessary between the two structures in this consideration, $\lambda = 0$ and $\lambda = 1$ can be different polymorphs of the same material (such as WZ and ZB structures of GaN) or different materials altogether (such as GaN and AlN); as long as they form an insulating interface, Eq. (5) will give the bound charge accumulation at the interface.

From the interface theorem [Eq. (5)] and Eq. (1), the bound polarization charge at the interface between different III-nitride materials (m and n) is

$$\begin{aligned} \sigma_b &= [P_{\text{SP}}^m + e_{31}^m(\epsilon_1^m + \epsilon_2^m) + e_{33}^m \epsilon_3^m] \\ &\quad - [P_{\text{SP}}^n + e_{31}^n(\epsilon_1^n + \epsilon_2^n) + e_{33}^n \epsilon_3^n]. \end{aligned} \quad (6)$$

As an example, we will take a realistic situation that occurs in heterostructures, by assuming that material n is strained coherently to m ($\epsilon_1^m = \epsilon_2^m = \epsilon_3^m = 0$), *i.e.*, under plane stress ($\epsilon_1^n = \epsilon_2^n, \epsilon_3^n = -2C_{13}^n/C_{33}^n \epsilon_1^n$, where C_{ij} are the elastic constants). Therefore we have

$$\begin{aligned} \sigma_b &= (P_{\text{SP}}^m - P_{\text{SP}}^n) - 2\epsilon_1^n(e_{31}^n - e_{33}^n C_{13}^n/C_{33}^n) \\ &= \Delta P_{\text{SP}}^{\text{int}} - 2\epsilon_1^n(e_{31}^n - e_{33}^n C_{13}^n/C_{33}^n). \end{aligned} \quad (7)$$

Note that σ_b is the charge density of electrons at an interface for which material n has been grown on top of material m in the $+c$ direction.

III. REFERENCE STRUCTURE FOR SPONTANEOUS POLARIZATION

A. Effective spontaneous polarization constants

We will first address the difference in spontaneous polarization in Eq. (7), $\Delta P_{\text{SP}}^{\text{int}}$. Strain effects will be taken into account separately in the PZ part, so that $\Delta P_{\text{SP}}^{\text{int}}$ is simply the difference of formal polarizations of the respective zero-strain structures,

$$\Delta P_{\text{SP}}^{\text{int}} = P_f^m|_{\epsilon=0} - P_f^n|_{\epsilon=0}. \quad (8)$$

For purposes of Eq. (1), we would like to define a SP polarization constant that is a property of a single material. Simply taking P_f^m of Eq. (8) as P_{SP}^m is problematic, since formal polarization is multivalued, being only well-defined modulo a quantum of polarization $e\mathbf{R}/\Omega$. Therefore, in every situation in which Eq. (1) is applied to determine σ_b at an interface, it must be confirmed that formal polarizations of the two materials are taken on the same “branch” of $e\mathbf{R}/\Omega$. A better approach is to take P_{SP}^m in Eq. (1) as a so-called “effective” SP polarization, \mathbf{P}_{eff} , defined by Resta and Vanderbilt [12] to be the $\Delta\mathbf{P}$ in Eq. (3) that results as the system is taken from a high-symmetry “reference” structure ($\lambda = 0$) to the structure of interest ($\lambda = 1$). That is,

$$\mathbf{P}_{\text{eff}} = \mathbf{P}_f^{(\lambda=1)} - \mathbf{P}_f^{(\lambda=0)} = \mathbf{P}_f - \mathbf{P}_f^{\text{ref}}. \quad (9)$$

Using \mathbf{P}_{eff} to define the SP polarization of the material removes the indeterminacy inherent to the formal polarization.

The reference structure is often chosen to be centrosymmetric, but it is important to recognize that the formal polarization of centrosymmetric crystals is not necessarily zero. This is because, as stated above, \mathbf{P}_f is a multivalued vector field, so it is possible for a nonzero formal polarization to be unchanged (modulo $e\mathbf{R}/\Omega$) under the inversion operator. Nevertheless, high symmetry puts restrictions on the possible values of $\mathbf{P}_f^{(\lambda=0)}$ [11].

While in principle effective polarization constants are still *differences* in formal polarization between $\lambda = 1$ and $\lambda = 0$ (reference) structures, in practice they can be used to compare spontaneous polarizations of different materials to obtain ΔP_{SP} if such materials share a reference structure with the same formal polarization. Such a comparison then correctly yields the interface charge density according to the interface theorem of Ref. 11. In such cases, ΔP_{SP} is just given by the difference in *effective* SP polarization of the materials,

$$\Delta \tilde{P}_{\text{SP}}^{\text{int}} = P_{\text{eff}}^m - P_{\text{eff}}^n. \quad (10)$$

In the more general case that the reference formal polarizations do not match, the correct change in SP polarization following from Eqs. (8) and (9) is

$$\Delta P_{\text{SP}}^{\text{int}} = \Delta \tilde{P}_{\text{SP}}^{\text{int}} + (P_f^{m,\text{ref}} - P_f^{n,\text{ref}}). \quad (11)$$

That is, a correction term of the form

$$\Delta P_{\text{corr}}^{\text{ref}} \equiv P_f^{m,\text{ref}} - P_f^{n,\text{ref}} \quad (12)$$

has to be added to Eq. (10). Unfortunately, this correction term is not typically implemented in device simulation packages (*e.g.*, Ref. 13) or used in the interpretation of experimental data (*e.g.*, Ref. 14, which is considered a standard reference in the field).

When the PZ terms are included as well, the total interface charge given by Eq. (7) becomes

$$\sigma_b = \Delta \tilde{P}_{\text{SP}}^{\text{int}} + \Delta P_{\text{corr}}^{\text{ref}} - 2\epsilon_1^n (e_{31}^n - e_{33}^n C_{13}^n / C_{33}^n). \quad (13)$$

Equation (13) is a central result of the present work.

B. Correction term for the effective spontaneous polarization with the zincblende reference structure

As mentioned before, previous studies [6–8] have exclusively used ZB (space group $F43m$) as a reference structure for calculating the SP polarization of the WZ. This structure is not centrosymmetric, although it has sufficient symmetry to preclude any SP polarization [1]. The fact that an insulating (111) interface can be constructed between the WZ and ZB polytypes [8] makes it an appropriate reference structure. In fact, experimental measurements have deduced the relative polarization between the WZ and ZB phases of GaN [5], which were found to be consistent with the theoretical values in Refs. 6–8.

However, there is a subtlety with using ZB as a reference structure: it has a nonzero formal polarization in the [111] direction, P_f^{ZB} (modulo $e\mathbf{R}/\Omega$). Again, this is consistent with the symmetry considerations because P_f is a multivalued vector quantity, and can be nonzero while still remaining unchanged (modulo $e\mathbf{R}/\Omega$) under the $F43m$ symmetry operations. These symmetry operations dictate the possible values of P_f^{ZB} , and therefore the resulting value depends only on the lattice constant, not on the chemical species of the atoms [11] (see Section S1 of the supplemental material (SM) [15] for more details on the formal polarization of ZB). The ZB reference structures for the reported effective SP polarization values for the III-nitrides were those with lattice constants equal to the in-plane lattice constant of the corresponding wurtzite material [6–8] (as confirmed by our calculations), so P_f^{ZB} will be *different* for GaN, AlN, and InN, and do not simply constitute a constant shift of P_f^{WZ} for all the materials. Therefore, for the effective SP polarization constants with the ZB reference to be implemented in Eq. (7) to determine the polarization difference between different WZ materials, the correction term of Eq. (12) is required, as in Eq. (13).

Consider the example of the interface charge between InN and GaN. Although, as mentioned above, the formal polarization of zincblende does not necessarily vanish, the symmetry of the structure severely limits the possible values. Specifically there are two possible values of the formal polarization in the [111] direction that are consistent with the symmetry: either P_f vanishes, or it is equal to $e\sqrt{3}/2a_n^2$ (both modulo $e\sqrt{2}a_n/\Omega_n$), where a_n is the WZ in plane lattice constant of material n and Ω_n is the volume of the ZB primitive cell (see Ref. 11 or Section S1 of the SM [15]). For the III-nitrides it is the latter, giving a correction term for GaN/InN:

$$\begin{aligned} \Delta P_{\text{corr}}^{(\text{ZB ref})} &= P_f^{\text{GaN,ZB}} - P_f^{\text{InN,ZB}} \\ &= \frac{e\sqrt{3}}{2} \left(\frac{1}{(a_{\text{GaN}})^2} - \frac{1}{(a_{\text{InN}})^2} \right) \\ &= 0.28 \text{ C/m}^2. \end{aligned} \quad (14)$$

When considering the SP polarization differences between WZ nitrides, this represents a significant correction. In fact, as we will show in Section III C, the correc-

tion is an order of magnitude larger than the effective polarizations when they are calculated with the zincblende reference [6, 7]. As we shall see later in Section V E, this error is substantially reduced in practice by an approximate error cancellation that occurs in connection with the treatment of the PZ response.

There is nothing intrinsically wrong with using ZB as the reference structure for defining WZ effective SP polarization; however if these values are to be used to obtain polarization differences between different WZ materials, the $\Delta P_{\text{corr}}^{\text{ref}}$ term [Eq. (12), or Eq. (14) for the example of GaN/InN] must be explicitly included in expressions such as Eq. (11) or Eq. (13). To our knowledge, however, this has not been properly implemented in the numerous previous evaluations of SP polarization for nitride interfaces, and it would require changes in the software for the many simulation tools that include modeling of polarization fields in heterostructures.

C. $P6_3/mmc$ hexagonal layered structure as an alternative reference

In order to avoid extensive changes in the simulation software, and to enhance physical insight, we advocate another approach, namely to determine effective SP polarization constants with respect to a reference structure for which the formal polarization is explicitly zero (so that $\Delta P_{\text{SP}}^{\text{int}} = \Delta \tilde{P}_{\text{SP}}^{\text{int}}$). A straightforward choice for this reference structure is the layered hexagonal (H) structure (space group $P6_3/mmc$), as was used for hexagonal $P6_3mc$ ABC materials [16]. This structure is centrosymmetric, and we will show below with explicit first-principles calculations that it remains insulating and its formal polarization vanishes. The layered hexagonal structure can be obtained by an adiabatic (gap preserving) increase of the internal structural u parameter from $u \approx 0.37 - 0.38$ of the WZ structure to $u = 0.5$. All that is required to avoid correction terms like Eq. (14) is to replace the effective SP polarization constants currently used in the field (the ones referenced to ZB [6, 7]) with those referenced to the H reference structure. We have explicitly verified that this leads to expressions that are identical to those that would be obtained for the ZB reference, provided the second term in Eq. (11) or Eq. (13) is included.

The first-principles calculations of P_f for the H, WZ, and ZB structures of the III-nitrides were performed using density functional theory with the screened hybrid functional of Heyd, Scuseria, and Ernzerhof (HSE) [17] as implemented in the VASP code [18]. Hartree-Fock mixing parameters of 31% for AlN and GaN, and 25% for InN were used to correctly describe the band gaps and structural parameters of each material. Conventional functionals based on the local density approximation (LDA) or generalized gradient approximation (GGA) predict InN to be a metal, precluding the calculation of the polarization constants if the Γ point is included in the k -

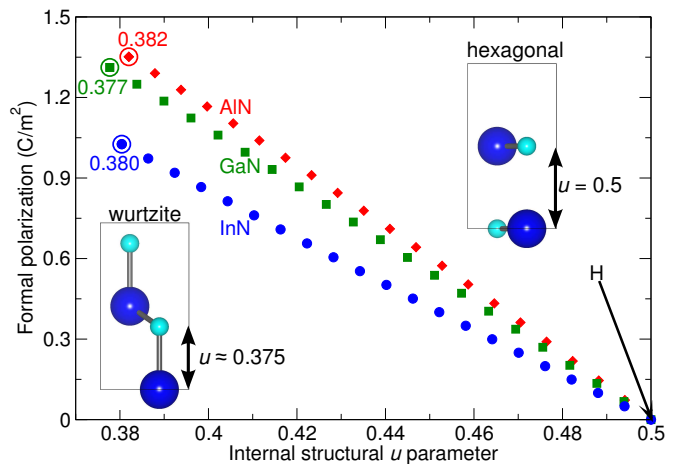


FIG. 1. Formal polarization of InN, GaN, and AlN for structures as a function of the internal structural parameter u , varying between fully relaxed WZ (circled symbols, labelled with relaxed u value) and H ($u = 0.5$), as shown schematically by ball and stick models where smaller balls represent N atoms and larger ones represent the cations. All other lattice parameters were fixed at their relaxed WZ values.

point mesh (which is required in VASP). Projector augmented wave potentials (PAW) [19], with the In and Ga d electrons frozen in the core, were used. All calculations were performed on bulk primitive cells, with a $6 \times 6 \times 8$ Monkhorst-Pack [20] k -point mesh to sample the Brillouin zone, and a large energy cutoff of 600 eV for the plane-wave basis set, chosen to ensure convergence of the internal structural parameter u . The calculated lattice parameters and band gaps, listed in Section S2 of the SM [15], show good agreement with experimental data.

We have calculated the electronic structure for structures with increasing u , ranging from $u \approx 0.37$ to $u = 0.5$ (Fig. 1), and confirmed that this path between WZ and H is gap preserving. These calculations also show that the formal polarization of the H structure is zero (modulo $e\mathbf{R}/\Omega$) for the III-nitrides (Fig. 1). We remind the reader that this was not guaranteed, since \mathbf{P}_f can be nonzero and still consistent with inversion symmetry, if the inversion operator changes \mathbf{P}_f by a multiple of $e\mathbf{R}/\Omega$. We have therefore verified that the hexagonal phase is a reference structure for which there is no spurious term in Eq. (11).

In addition, by correcting for any discontinuities (in the amount of a multiple of $e\mathbf{R}/\Omega$) that may occur in the calculations of formal polarizations along the path between WZ and H, we have insured that we are comparing formal polarizations of WZ GaN, AlN, InN on the same branch of $e\mathbf{R}/\Omega$ [12].

The calculated spontaneous polarization coefficients for the WZ structure using either H or ZB as a reference are given in Table I. The results obtained by Bernardini *et al.* [6, 7] are listed for comparison. The GGA functional used in that work provides results that are very close to those we obtained with HSE; the discrepancy is the largest for InN, which is probably related to the

TABLE I. Effective spontaneous polarization constants in units of C/m^2 of wurtzite (WZ) GaN, AlN, and InN calculated using either the hexagonal (H, space group $P6_3/mmc$) or zincblende (ZB, space group $F\bar{4}3m$) reference structures. The lattice constant of the ZB structure is chosen to match the in-plane lattice constant of the WZ structure for the same material. Results from previous calculations [7] that used the ZB reference are listed for comparison.

	$P_{\text{eff}}^{(\text{H ref})}$	$P_{\text{eff}}^{(\text{ZB ref})}$	$P_{\text{eff}}^{(\text{ZB ref})}$, prev. ^a
GaN	1.312	-0.035	-0.034
AlN	1.351	-0.090	-0.090
InN	1.026	-0.053	-0.042

^a From Ref. 7.

fact, mentioned above, that GGA predicts InN to be a metal. Table I also shows, however, that the choice of reference structure makes a significant difference. The magnitudes of the coefficients are much larger, and their signs are different when H is used as the reference. We observe that it is not just the absolute values, but also the relative differences between the calculated polarization constants of the three materials that differ from the previously reported values [6, 7].

The difference in sign of $P_{\text{eff}}^{(\text{H ref})}$ compared to $P_{\text{eff}}^{(\text{ZB ref})}$ demonstrates that the conventional wisdom that the SP polarization in WZ points in the $-c$ direction is misleading. The formal polarization of WZ has no definite sign as this would depend on the chosen branch. The effective SP depends on the polarization difference, and therefore the sign will depend on the sign and magnitude of the formal polarization of the reference structure.

Even though the values reported in Table I for $P_{\text{eff}}^{(\text{H ref})}$ and $P_{\text{eff}}^{(\text{ZB ref})}$ clearly differ in sign, absolute magnitude, and relative differences between materials, we will show in Section V that the final predictions based on both formulations are actually rather similar, because of the way the PZ contributions have been included in the previous work (*cf.* Section IV).

IV. IMPROPER VERSUS PROPER PIEZOELECTRIC CONSTANTS

We now address the specifics of the PZ terms in Eqs. (7) and (13). A complication that must be addressed is the choice between improper and proper e_{31} (e_{33} has no such complication) [2, 4].

As we have done above, consider a thin layer of a WZ material grown in the c direction. If the layer is strained perpendicular to the c direction, the total bound charge on the $+c$ and $-c$ surfaces will change as a result of the polarization current, or redistribution of charge, in the layer. If metallic contacts on the $+c$ and $-c$ surfaces are short-circuited when the strain occurs, the current flow can be measured directly and will give the proper PZ constant, denoted e_{31}^{prop} [2, 4].

If the $+c$ and $-c$ faces are in open-circuit boundary conditions, the layer will have a field across it due to the SP polarization, which will be modified by the strain via two mechanisms. The first is the same as in the proper case, as the strain will cause a flow of polarization current. But in addition, since the field depends on the charge *density*, the change in the area of the c -plane as a result of ϵ_1 will dilute or concentrate the pre-strain bound charge. For small strains the latter is given by the zero-strain formal polarization [2, 4]. Taking both of these mechanisms into account gives the improper PZ constant, e_{31}^{imp} .

In the case of, *e.g.*, Eq. (13), the PZ constants correspond to the improper case, since their role in the equation is to take into account the change in formal polarization of material n with strain, so that σ_b corresponds to the bound charge at the coherent interface with the in-plane lattice constant of material m . The change in formal polarization with strain is an alternative definition of the improper PZ constants [4].

From Refs. 2 and 4, the improper PZ constant $e_{31}^{n,\text{imp}}$ is related to the proper constant by

$$e_{31}^{n,\text{imp}} = e_{31}^{n,\text{prop}} - P_f^n|_{\epsilon=0}, \quad (15)$$

where $P_f^n|_{\epsilon=0}$ is the zero-strain formal polarization of material n . There is no change to the e_{33} PZ constant. The proper PZ constant is a well-defined bulk quantity, as it is related to the polarization current; however the improper PZ constant is branch dependent [4]. Here also, defining polarization with respect to the H reference proves useful. Since the formal polarization of the H structure vanishes (Fig. 1), $P_{\text{eff}}^{n,(\text{H ref})} = P_f^{n,\text{WZ}}|_{\epsilon=0}$; this also ensures that improper PZ constants for the different materials are taken on the same branch, in the same way as this is confirmed for the SP polarization constants. Therefore, consistent use of the H reference structure allows us to write Eq. (7) as

$$\sigma_b = \Delta \tilde{P}_{\text{SP}}^{\text{int},(\text{H ref})} - 2\epsilon_1^n \left(e_{31}^{n,\text{prop}} - P_{\text{eff}}^{n,(\text{H ref})} - e_{33}^{n,\text{prop}} C_{13}^n / C_{33}^n \right), \quad (16)$$

where $P_{\text{eff}}^{n,(\text{H ref})}$ can be taken from Table I.

TABLE II. Calculated piezoelectric polarization constants in units of C/m^2 compared with reported values from the literature.

		proper	improper	prev. reported ^a
GaN	e_{31}	-0.551	-1.863	-0.22 to -0.55
	e_{33}	1.020	1.020	0.43 to 1.12
AlN	e_{31}	-0.676	-2.027	-0.38 to -0.81
	e_{33}	1.569	1.569	1.29 to 1.94
InN	e_{31}	-0.604	-1.63	-0.23 to -0.59
	e_{33}	1.238	1.238	0.39 to 1.09

^a From Ref. 3 and references therein.

Calculated proper PZ constants are given in the “proper” column of Table II. Since the HSE hybrid functional was used (and therefore density functional perturbation theory was not implemented), finite differences were used to calculate the derivatives with strain, following the procedure outlined in Eqs. (4)-(6) in Ref. 6. Specifically, improper PZ constants were calculated, and converted to proper constants by adding $P_f^n|_{\epsilon=0}$ [see Eq. (15)] as determined in the calculation. This removes any dependence on the branch choice used in finite-difference calculations [4]. We then convert *back* to improper constants using $P_{\text{eff}}^{n,(\text{H ref})}$ as discussed above, in order to ensure that the constants are reported for the same branch for each material (“improper” column in Table II).

The WZ structure does have another nonzero piezoelectric constant e_{15} , which couples a shear deformation in a plane perpendicular to the c plane (ϵ_{13} or ϵ_{31}) to the polarization in the c plane. In this case, there are two improper PZ constants, since a correction must be included in the case of ϵ_{13} but not for ϵ_{31} [4]. These elements do not enter in the situation we consider in this work (plane stress conditions with the c plane as the growth plane), but may be important for growth on nonpolar or semipolar planes [21].

It is important to comment on the PZ constants reported in the literature [3]. When PZ polarization constants have been implemented in simulations (*e.g.* Refs. 3, 13, and 14) it has never been specified *which* PZ constants are used for WZ III-nitrides. However, by comparing our calculations of proper and improper PZ constants (“proper” and “improper” columns of Table II) with the reported PZ constants in the literature (“prev. reported” of Table II) we have found that the reported constants are more likely to be the proper PZ constants.

From an experimental perspective, most of the experimental techniques have measured *total* polarization, and then deduced the PZ constants in the nitrides using the SP constants from, *e.g.*, Ref. 6 using Eq. 1. As we will show in Section V, observation of the effects of total polarization can be misleading with regards to the differentiation between proper and improper PZ constants, due to the error cancellation from the use of the ZB reference in defining the SP polarization (discussed in Section IIIB).

There have been direct measurements of the PZ constants, either by probing the electromechanical coupling constants via surface acoustic waves [22, 23], or by using interferometry to determine the strain caused by the application of a voltage [24–27]. Both of these techniques measure the *proper* constants, since neither is sensitive to the change in surface charge density resulting from the deformation. These reported values indeed agree well with our calculated values for the proper PZ constants, both in sign and in magnitude.

In previous work [7], $P_{\text{eff}}^{n,(\text{ZB ref})}$ was used instead of $P_f^n|_{\epsilon=0}$ in Eq. (15) to convert improper to proper e_{31} PZ

constants (*cf.* Table VI and V of Ref. 7). Because of the nonvanishing formal polarization of the ZB reference structure, $P_{\text{eff}}^{n,(\text{ZB ref})} \neq P_f^{n,\text{WZ}}|_{\epsilon=0}$; instead, we see from the discussion resulting in Eq. (14) that Eq. (15) can be expressed as

$$e_{31}^{n,\text{imp}} = e_{31}^{n,\text{prop}} - \left(P_{\text{eff}}^{n,\text{ZB ref}} + \frac{e\sqrt{3}}{2a_n^2} \right), \quad (17)$$

where a_n is the equilibrium, in-plane lattice constant of the WZ material n . To our knowledge the inclusion of the last term in Eq. (17) has not been discussed in the literature. Because of the small magnitude of $P_{\text{eff}}^{n,(\text{ZB ref})}$, neglecting the last term in Eq. (17) led to the conclusion in Ref. 7 that the difference between the proper and improper PZ constants is small, seemingly rendering the distinction of no consequence. Instead, because of the large magnitude of $P_{\text{eff}}^{n,(\text{H ref})}$ [and $e\sqrt{3}/2a_n^2$ in Eq. (17)], the distinction between proper and improper PZ constants is actually very significant.

V. COMPARISON WITH REPORTED EXPERIMENTAL RESULTS

A. Correct expressions for total polarization for wurtzite materials

Before discussing specific quantitative results for nitride semiconductors, we briefly summarize the main points of the previous sections and rigorously express the polarization of a given WZ material [Eq. (1)]. Spontaneous polarization constants must be defined with respect to a reference structure, and this choice of reference structure must be taken into account when evaluating polarization discontinuities at interfaces. We determined a correction term [Eq. (12)] that is necessary when effective SP polarization constants are used to determine the SP polarization difference between materials at an interface. This correction term is significant when the ZB reference structure is used [*e.g.*, Eq. (14)], but is zero for the H reference. Using H as a reference is therefore more straightforward and is the approach we advocate, with the SP constants $P_{\text{eff}}^{(\text{H ref})}$ listed in Table II.

In addition, the improper PZ constants should be used to determine interface bound charge and fields in heterostructure layers. These can be obtained from the proper constant e_{31}^{prop} by subtracting $P_{\text{eff}}^{(\text{H ref})}$ (Table II). Therefore, in the notation of this paper, Eq. (1) is written rigorously as

$$P = P_{\text{eff}}^{(\text{H ref})} + (\epsilon_1 + \epsilon_2) \left(e_{31}^{\text{prop}} - P_{\text{eff}}^{(\text{H ref})} \right) + \epsilon_3 e_{33}^{\text{prop}}. \quad (18)$$

B. Calculation of sheet charges for III-nitrides

Because of the important impact of polarization on device performance and design, a plethora of experimental

studies have been aimed at determining the effects of polarization at GaN/InGaN and GaN/AlGaN heterostructures. We have plotted these reported results in Fig. 2, expressed as the magnitude of polarization bound charge at the interface, as a function of alloy content (a full list of references is provided in Section S3 of the SM [15]).

For GaN grown in the $+c$ direction with the InGaN (AlGaN) grown on top, the sign of the bound charge at the interface will be negative (positive) [28].

In Fig. 2, the black dashed curves correspond to the current practice in the field: sheet charges are predicted based on (i) SP constants referenced to the ZB structure ($P_{\text{eff}}^{(\text{ZB ref})}$ in Table I) and Eq. (13) *without* the correction term $\Delta P_{\text{corr}}^{(\text{ZB ref})}$; and (ii) proper PZ constants (“proper” column in Table II). Quantities for alloys were obtained using linear interpolation. For an explicit expression in terms of alloy content, see Eq. (3) in Section S4 of the SM [15]. Elastic constants were taken from Ref. 29.

The red solid line in Fig. 2 corresponds to the implementation recommended in this work, *i.e.*, using the H reference structure and the improper PZ constants, as in Eqs. (16) and (18) [and Eq. (5) in Section S4 of the SM [15]].

In view of the arguments given above, it may seem surprising that the dashed black and solid red curves agree as well as they do; we will return to this point in Section V E.

C. InGaN/GaN interfaces

For the InGaN/GaN system, most experimental studies have applied optical techniques to determine the polarization fields in GaN/InGaN/GaN quantum wells (QWs). This field can be probed by varying QW width [30] or external biases [31] and measuring the change in the optical properties of the QW (labeled “optical” in Fig. 2). In addition, there have also been studies using time-resolved PL to measure shifts due to screening of the polarization field by photoexcited or electrically injected carriers [32]. Other studies have been based on electron holography [33], where cross-sectional transmission electron microscopy is conducted on InGaN/GaN heterostructures to determine the depth-resolved electrostatic potential in the growth direction, and capacitance-voltage (CV) profiling of the fields [34]. When fields are reported, we convert to bound charge for the purposes of Fig. 2(a), assuming GaN/InGaN/GaN quantum well (with thick barriers such that the electric field in the barriers is presumed zero) using a simple parallel-plate capacitor model ($E = \sigma/\epsilon_0\epsilon_r$, using a relative dielectric constant for GaN of 10 [35] and for InN of 15 [36] and a linear interpolation for the dielectric constant of InGaN). For specific values of the points in Fig. 2, see Section S3 of the SM [15].

The red curve in Fig. 2(a) is indeed in reasonable agreement with the experimental observations, appearing to be an upper bound of the data. The optical experiments

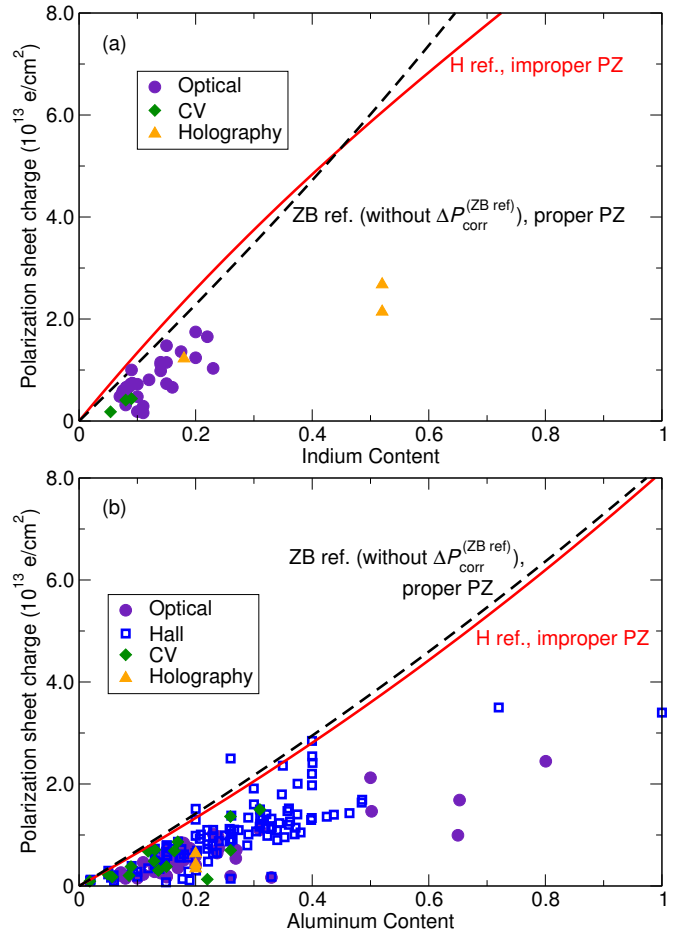


FIG. 2. Absolute values for polarization sheet charges at the (a) InGaN/GaN and (b) AlGaN/GaN interface as a function of alloy content predicted from the spontaneous polarization constants calculated using either the zincblende (ZB) reference structure [without correction term, Eq. (14)] and the proper piezoelectric constants (black dashed curve), or the hexagonal (H) reference structure and improper piezoelectric constants (red solid curve). Points are experimental values from the literature (see Section S3 of the SM [15] for references and values).

usually rely on Schrödinger-Poisson simulations to determine the field magnitude from the measured optical properties. Uncertainties in input parameters to these models such as well widths, compositions, and composition profiles can result in quantitative differences. It has been shown recently that taking into account the deviations from an ideal QW structures when interpreting experimental observations can account for the apparent discrepancy between the measurements and theoretical prediction of polarization fields [37, 38]. Such deviations are expected to be significant for InGaN/GaN because of the large lattice mismatch and the large difference in optimal growth temperatures for GaN and InGaN.

D. AlGa_n/Ga_n interfaces

For the AlGa_n/Ga_n system, there are two basic strategies for experimentally determining polarization effects. The first is to directly measure the polarization field in an AlGa_n/Ga_n/AlGa_n (QW) structure with the same methods as used in the InGa_n/Ga_n case [39, 40]. For the purposes of Fig. 2(b) we have converted these fields to bound sheet charge densities in an AlGa_n/Ga_n/AlGa_n quantum well (using a relative dielectric constant for Ga_n of 10 [35]).

The other strategy is to measure the density of the 2DEG at the AlGa_n/Ga_n interface in a HEMT structure (Ga_n channel, AlGa_n barrier); from this, the bound interface charge, σ_b , can be derived [41]. The 2DEG density can be determined either by Hall effect [14] or CV [41] measurements.

The significant scatter in the experimental data in Fig. 2(b) may have several origins. There are experimental uncertainties that can influence fields, such as incomplete strain relaxation in buffer layers [42], and differences in background doping [43–45].

As in the case of InGa_n/Ga_n, the predicted sheet charges appear to be an overestimation compared to the experimental observations. In the case of optical measurements, Schrödinger-Poisson modeling is again typically used to interpret the measured properties, and the same uncertainties and systematic errors may arise as discussed in the case of InGa_n/Ga_n [46, 47]. For the cases where the compensating 2DEG density is measured, the thickness of the AlGa_n layer and Schottky barrier height at the AlGa_n surface will determine whether the entire bound charge is compensated, which could be a reason that the observations are slightly lower than predicted theoretically [48]. Also, interface roughness and electron traps due to dislocations and/or surface states have been proposed to explain the reduced 2DEG density [14].

E. Comparison of theoretical implementations

The degree of agreement between results obtained based on the current practice in the field (ZB reference, no correction term, proper PZ) and our revised implementation (H reference, improper PZ constants) merits some discussion. It is clear from Table I that the SP polarization values determined with the H reference structure are very different from those determined with the ZB reference; also, from Table II, the improper and proper e_{31} coefficients are very different. However, the similarity between the red solid and black dashed curves in Fig. 2 demonstrates that these two large corrections cancel when we evaluate Eq. (18). I.e., the correct implementation (H reference, improper PZ constants) results in values that are only slightly different from the current (incorrect) practice in the field (ZB reference, no correction term, proper PZ). We now demonstrate analytically how this accidental agreement comes about.

If we take the difference between our revised implementation (solid red curve in Fig. 2) and the current practice in the field (dashed black curve in Fig. 2) for a given x , we obtain the total error in using the current practice in the field:

$$\Delta P_{\text{error}} = x \Delta P_{\text{corr}}^{(\text{ZB ref})} + 2\epsilon_1(x) P_{\text{eff}}^{n,(\text{H ref})}(x). \quad (19)$$

A derivation of this expression is given in Section S5 of the SM [15]. For both AlGa_n/Ga_n and InGa_n/Ga_n, the two terms on the right-hand side of Eq. (19) have opposite signs and a tendency to cancel. To understand why, first note that $\epsilon_1(x)$ is approximately linear in x , so that both terms can be regarded as being roughly proportional to $\epsilon_1(x)$. In particular, linearizing Eq. (14) in ϵ_1 , we find $x \Delta P_{\text{corr}}^{(\text{ZB ref})} \simeq -2\epsilon_1(x) P_{\text{f}}^{m,\text{ZB}}$ [see also Eq. (8) of the SM [15]]. Thus

$$\begin{aligned} \Delta P_{\text{error}} &\simeq 2\epsilon_1(x) \left(P_{\text{eff}}^{n,(\text{H ref})} - P_{\text{f}}^{m,\text{ZB}} \right) \\ &= 2\epsilon_1(x) \left(P_{\text{f}}^{n,\text{WZ}} - P_{\text{f}}^{m,\text{ZB}} \right) \\ &= 2\epsilon_1(x) \left[P_{\text{eff}}^{n,\text{ZB ref}} + \left(P_{\text{f}}^{n,\text{ZB}} - P_{\text{f}}^{m,\text{ZB}} \right) \right], \end{aligned} \quad (20)$$

where in the second step we used the fact that the formal polarization of the H structure vanishes. For the III-nitrides, $|\epsilon_1| < 0.1$, and we see from Table I that $|P_{\text{eff}}^{n,\text{ZB}}| < 0.1 \text{ C/m}^2$. The second term in the last line of Eq. (20), $P_{\text{f}}^{n,\text{ZB}} - P_{\text{f}}^{m,\text{ZB}}$, is related to the difference in in-plane lattice constants between material n and material m (Section III B). The largest value it will take for the materials considered in this study is 0.28 C/m^2 for InN on GaN, as calculated in Eq. (14), and it will be significantly smaller for lower alloy content and for the case of AlGa_n on Ga_n. The error is therefore the product of small factors, and thus small in practice, significantly smaller than the errors in the SP and PZ parts individually.

The small magnitude of $P_{\text{eff}}^{n,\text{ZB}}$ (Table I) demonstrates that $P_{\text{f}}^{\text{WZ}} \sim P_{\text{f}}^{\text{ZB}}$ in these materials (see Section S1 of the SM [15]). The similarity between P_{f}^{ZB} and P_{f}^{WZ} is not unexpected. Although ZB has sufficient symmetry to preclude SP polarization, in the [111] direction the structure only differs from the WZ c direction by the stacking of the cation/anion planes and a small deviation from the ideal WZ u parameter and c/a lattice constants. In WZ materials other than the III-nitrides, such deviations could in principle be larger, and in that case $P_{\text{eff}}^{\text{ZB ref}}$ will be larger, resulting in ΔP_{error} being more significant.

For AlGa_n/Ga_n, the relatively modest difference in lattice constants between AlN and GaN (and therefore modest ϵ_1 values for coherently strained alloy layers), and an almost exact cancellation between $P_{\text{f}}^{\text{Ga_n,ZB}}$ and $P_{\text{eff}}^{\text{AlGa_n,(\text{H ref})}}$ means that the difference between implementations is small over the whole composition range (c_f Section S5 of the SM [15]). For InGa_n/Ga_n, the large lattice mismatch of InN and GaN and a less complete cancellation of $P_{\text{f}}^{\text{Ga_n,ZB}}$ and $P_{\text{eff}}^{\text{InGa_n,(\text{H ref})}}$ results

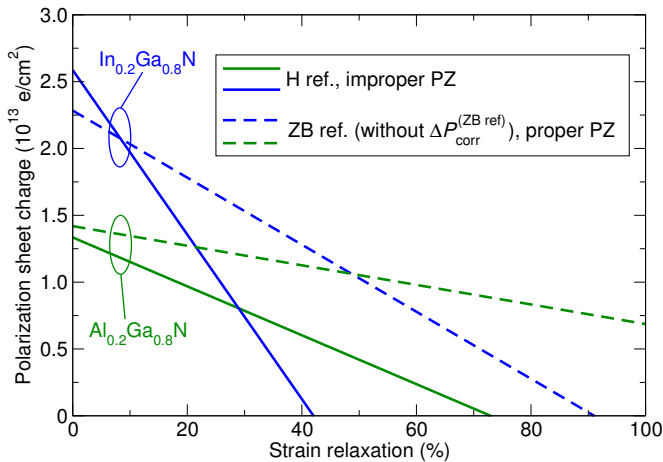


FIG. 3. Absolute values for polarization sheet charges at the $\text{In}_{0.2}\text{Ga}_{0.8}\text{N}/\text{GaN}$ (blue) and $\text{Al}_{0.2}\text{Ga}_{0.8}\text{N}/\text{GaN}$ (green) interface as a function of percent strain relaxation. 0 % relaxation corresponds to perfectly strained layers, 100 % relaxation to an unstrained overlayer at its bulk lattice constant. Solid curves are the correct implementation described in this work (H reference for SP and improper PZ constants); dashed curves are the current practice in the field (ZB reference for SP, without the correction term, and proper PZ constants).

in a significant deviation at higher In content; this will be important for the prediction of polarization fields in applications such as tunnel field-effect transistors based on thin, high In-content interlayers [49].

The two implementations differ significantly in the *relative* contributions of SP and PZ polarization. An effect of this is illustrated by the case where there is strain relaxation in the alloy layer. In Fig. 3 the predicted polarization bound charges for $\text{In}_{0.2}\text{Ga}_{0.8}\text{N}/\text{GaN}$ (blue curves) and $\text{Al}_{0.2}\text{Ga}_{0.8}\text{N}/\text{GaN}$ (green curves) are shown as a function of strain relaxation of the layer, modeled by simply scaling ϵ_1 . For both InGaN/GaN and AlGaIn/GaN , the revised implementation of this work predicts a much faster decrease in bound charge at the interface than the current practice in the field. Of course, strain relaxation is associated with the presence of edge dislocations at the interface, which may themselves influ-

ence the interface bound charge; this effect has not been taken into account in either version of the implementation.

VI. CONCLUSIONS

We have derived a rigorously correct implementation of polarization constants in wurtzite materials, focusing on the example of the III-nitrides. Our derivation has demonstrated the impact of the choice of reference structure when calculating spontaneous polarization constants using the modern theory of polarization. Insufficient care in using the values can result in spurious contributions to the polarization discontinuities at heterostructure interfaces. We have provided new values calculated with a consistent hexagonal (rather than zincblende) reference structure. In addition, we have demonstrated the importance of choosing the correct piezoelectric constants (improper), and provided values for these improper constants. These revised values of the spontaneous and piezoelectric constants can be directly used in simulations and to interpret experimental observations. The revised implementation predicts a more rapid decrease of polarization charge with strain relaxation for an alloy layer on GaN.

ACKNOWLEDGMENTS

Work by C. E. D. was supported by the U.S. Department of Energy (DOE), Office of Science, Basic Energy Sciences (BES) under Award de-sc0010689. Work by A. J. was supported by the Center for Low Energy Systems Technology (LEAST), one of the six SRC STARnet Centers, sponsored by MARCO and DARPA. Work by D. V. was supported by ONR Grant N00014-12-1-1035. Computational resources were provided by the CSC at the CNSI and MRL (an NSF MRSEC, DMR-1121053) (NSF CNS-0960316) and by the National Energy Research Scientific Computing Center, a DOE Office of Science User Facility supported by the Office of Science of the U.S. Department of Energy under Contract No. DE-AC02-05CH11231.

[1] J. F. Nye (1957). *Physical Properties of Crystals* (pp. 300). London: Oxford University Press.
 [2] R. M. Martin, *Piezoelectricity*, Phys. Rev. B **5**, 1607 (1972).
 [3] M. Feneberg and K. Thonke, *Polarization fields of III-nitrides grown in different crystal orientations*, J. Phys.: Condens. Matter **19**, 403201 (2007).
 [4] D. Vanderbilt, *Berry-phase theory of proper piezoelectric response*, J. Phys. Chem. Sol. **61**, 147 (2000).
 [5] J. Lähnemann, O. Brandt, U. Jahn, C. Pfüller, C. Roder, P. Dogan, F. Grosse, A. Belabbes, F. Bechstedt, A.

Trampert, and L. Geelhaar, *Direct experimental determination of the spontaneous polarization of GaN*, Phys. Rev. B **86**, 081302 (2012).
 [6] F. Bernardini, V. Fiorentini, D. Vanderbilt, *Spontaneous polarization and piezoelectric constants of III-V nitrides*, Phys. Rev. B **56**, R10024 (1997).
 [7] F. Bernardini, V. Fiorentini, D. Vanderbilt, *Accurate calculation of polarization-related quantities in semiconductors*, Phys. Rev. B **63**, 193201 (1997).
 [8] F. Bechstedt, U. Grossner, and J. Furthmüller, *Dynamics and polarization of group-III nitride lattices: A first-*

- principles study*, Phys. Rev. B **62**, 8003 (2000).
- [9] R. D. King-Smith and D. Vanderbilt, *Theory of polarization of crystalline solids*, Phys. Rev. B **47**, 1651 (1993).
- [10] R. Resta, *Macroscopic polarization in crystalline dielectrics: the geometric phase approach*, Rev. Mod. Phys. **66**, 899 (1994).
- [11] D. Vanderbilt and R. D. King-Smith, *Electric polarization as a bulk quantity and its relation to surface charge*, Phys. Rev. B **48**, 4442 (1993).
- [12] R. Resta and D. Vanderbilt, in *Physics of Ferroelectrics: A Modern Perspective*, edited by K. Rabe, Ch. H. Ahn, and J.-M. Triscone (Springer-Verlag, Berlin, 2007).
- [13] SiLENSe Physics Summary v5.2 (2011).
- [14] O. Ambacher, B. Foutz, J. Smart, J. R. Shealy, N. G. Weimann, K. Chu, M. Murphy, R. Dimitrov, A. Mitchell, and M. Stutzmann, *Two dimensional electron gases induced by spontaneous and piezoelectric polarization in undoped and doped AlGaIn/GaN heterostructures*, J. Appl. Phys. **87**, 334 (2000).
- [15] See Supplemental Material at [URL will be inserted by publisher] for a discussion of formal polarization in ZB, a table of structural properties and band gaps, a list of experimental references, equations used to generate curves in Fig. 2, and equations demonstrating the difference between implementations.
- [16] J. W. Bennett, K. F. Garrity, K. M. Rabe, and D. Vanderbilt, *Hexagonal ABC Semiconductors as Ferroelectrics*, Phys. Rev. Lett. **109**, 167602 (2012).
- [17] J. Heyd, G. E. Scuseria, M. Ernzerhof, *Hybrid functionals based on a screened Coulomb potential*, J. Chem. Phys. **118**, 8207 (2003); *ibid.* **124**, 219906 (2006).
- [18] G. Kresse and J. Furthmüller, *Efficient iterative schemes for ab initio total-energy calculations using a plane-wave basis set*, Phys. Rev. B. **54**, 11169 (1996).
- [19] P. E. Blöchl, *Projector augmented-wave method*, Phys. Rev. B **50**, 17953 (1994).
- [20] H.J. Monkhorst, J. D. Pack, *Special points for Brillouin-zone integrations*, Phys. Rev. B **13**, 5188 (1976).
- [21] A. E. Romanov, T. J. Baker, S. Nakamura, and J. S. Speck, *Strain-induced polarization in wurtzite III-nitride semipolar layers*, J. Appl. Phys. **100**, 023522 (2006).
- [22] G. D. O'Clock and M. T. Duffy, *Acoustic surface wave properties of epitaxially grown aluminum nitride and gallium nitride on sapphire*, Appl. Phys. Lett. **23**, 55 (1973).
- [23] M.-A. Dubois and P. Muralt, *Properties of aluminum nitride thin films for piezoelectric transducers and microwave filter applications*, Appl. Phys. Lett. **74**, 3032 (1999).
- [24] S. Muensit and I. L. Guy, *The piezoelectric coefficient of gallium nitride thin films*, Appl. Phys. Lett. **72**, 1896 (1998).
- [25] S. Muensit, E. M. Goldys, and I. L. Guy, *Shear piezoelectric coefficients of gallium nitride and aluminum nitride*, Appl. Phys. Lett. **75**, 3965 (1999).
- [26] I. L. Guy, S. Muensit and E. M. Goldys, *Extensional piezoelectric coefficients of gallium nitride and aluminum nitride*, Appl. Phys. Lett. **75**, 4133 (1999).
- [27] C. M. Lueng, H. L. W. Chan, C. Surya, and C. L. Choy, *Piezoelectric coefficient of aluminum nitride and gallium nitride*, J. Appl. Phys. **88**, 5360 (2000).
- [28] O. Ambacher, R. Dimitrov, M. Stutzmann, B. E. Foutz, M. J. Murphy, J. A. Smart, J. R. Shealy, N. G. Weimann, K. Chu, M. Chumbes, B. Green, A. J. Sierakowski, W. J. Schaff, and L. F. Eastman, *Two-dimensional electron gases induced by spontaneous and piezoelectric polarization charges in N- and Ga-face AlGaIn / GaN heterostructures*, Phys. status solidi (b) **216**, 381 (1999).
- [29] I. Vurgaftman and J. R. Meyer, *Band parameters for nitrogen-containing semiconductors*, J. Appl. Phys. **94**, 3675 (2003).
- [30] A. Hangleiter, F. Hitzel, S. Lahmann, and U. Rossow, *Composition dependence of polarization fields in GaInN/GaN quantum wells*, Appl. Phys. Lett. **83**, 1169 (2003).
- [31] F. Renner, P. Kiesel, G. H. Döhler, M. Kneissl, C. G. Van de Walle, and N. M. Johnson, *Quantitative analysis of the polarization fields and absorption changes in InGaInN/GaN quantum wells with electroabsorption spectroscopy*, Appl. Phys. Lett. **81**, 490 (2002).
- [32] D. Turchinovich, P. Uhd Jepsen, B. S. Monozon, M. Koch, S. Lahmann, U. Rossow, and A. Hangleiter, *Ultrafast polarization dynamics in biased quantum wells under strong femtosecond optical excitation*, Phys. Rev. B **68**, 241307 (2003).
- [33] D. Cherns, J. Barnard, and F. A. Ponce, *Measurement of the piezoelectric field across strained InGaInN/GaN layers by electron holography*, Solid State Commun. **111**, 281 (1999).
- [34] H. Zhang, E. J. Miller, E. T. Yu, C. Poblenz, and J. S. Speck, *Analysis of interface electronic structure in In_xGa_{1-x}N/GaN heterostructures*, J. Vac. Sci. Technol. B **22**, 2169 (2004).
- [35] A. S. Barker, M. Ilegems, *Infrared Lattice Vibrations and Free-Electron Dispersion in GaN*, Phys. Rev. B **7**, 743 (1973).
- [36] O. Madelung, *Semiconductors: Data Handbook* (Springer Berlin Heidelberg, 2004).
- [37] Y.-R. Wu, R. Shivaraman, K.-C. Wang, and J. S. Speck, *Analyzing the physical properties of InGaIn multiple quantum well light emitting diodes from nano scale structure*, Appl. Phys. Lett. **101**, 083505 (2012).
- [38] P. M. McBride, Q. Yan, and C. G. Van de Walle, *Effects of In profile on simulations of InGaIn / GaN multiple quantum-well light-emitting diodes*, Appl. Phys. Lett. **105**, 083507 (2014).
- [39] N. Grandjean, B. Damilano, S. Dalmaso, M. Leroux, M. Lügt, and J. Massies, *Built-in electric-field effects in wurtzite AlGaIn/GaN quantum wells*, J. Appl. Phys. **86**, 3714 (1999).
- [40] M. Leroux, N. Grandjean, J. Massies, B. Gil, P. Lefebvre, and P. Bigenwald, *Barrier-width dependence of group-III nitrides quantum-well transition energies*, Phys. Rev. B **60**, 1496 (1999).
- [41] E. T. Yu, G. J. Sullivan, P. M. Asbeck, C. D. Wang, D. Qiao, and S. S. Lau, *Measurement of piezoelectrically induced charge in GaN/AlGaIn heterostructure field-effect transistors*, Appl. Phys. Lett. **71**, 2794 (1997).
- [42] Y. Zhou, B. Shen, T. Someya, H. Yu, J. Liu, H. Zhou, R. Zhang, Y. Shi, Y. Zheng, and Y. Arakawa, *Investigation of the polarization-induced charges in modulation-doped Al_xGa_{1-x}N/GaN heterostructures through capacitance-voltage profiling and simulation*, Jpn. J. Appl. Phys. **41**, 2531 (2002).
- [43] K. Köhler, S. Müller, P. Waltereit, W. Pletschen, V. Polyakov, T. Lim, L. Kirste, H. P. Menner, P. Brückner, O. Ambacher, C. Buchheim, and R. Goldhahn, *Electrical properties of Al_xGa_{1-x}N/GaN heterostructures with low Al content*, J. Appl. Phys. **109**, 053705 (2011).

- [44] S. K. Davidsson, M. Gurusinge, T. G. Andersson, H. Zirath, *The influence of composition and unintentional doping on the two-dimensional electron gas density in AlGaN/GaN heterostructures*, J. Electron. Mater. **33**, 440 (2004).
- [45] J. Simon, R. Langer, A. Barski, M. Zervos, and N. T. Pelekanos, *Residual doping effects on the amplitude of polarization-induced electric fields in GaN/AlGaN quantum wells*, Phys. Stat. Sol. (a) **188**, 867 (2001).
- [46] S. Arulkumaran, T. Egawa, H. Ishikawa, and T. Jimbo, *Characterization of different Al content $Al_xGa_{1-x}N$ heterostructures and high-electron-mobility transistors on sapphire*, J. Vac. Sci. Technol. B **21**, 888 (2003).
- [47] K. A. Mkhoyan, J. Silcox, Z. Yu, W. J. Schaff, L. F. Eastman, *Formation of a quasi-two-dimensional electron gas in GaN/ $Al_xGa_{1-x}N$ heterostructures with diffuse interfaces*, J. Appl. Phys. **95**, 1843 (2004).
- [48] Y. Zhang, I. P. Smorchkova, C. R. Elsass, S. Keller, J. P. Ibbetson, S. P. DenBaars, U. K. Mishra, J. Singh, *Charge control and mobility in AlGaIn/GaN transistors: Experimental and theoretical studies*, J. Appl. Phys. **87**, 7981 (2000).
- [49] W. Li, S. Sharmin, H. Ilatikhameneh, R. Rahman, Y. Lu, J. Wang, X. Yan, A. Seabaugh, G. Klimeck, D. Jena, and P. Fay, *Polarization-Engineered III-Nitride Heterojunction Tunnel Field-Effect Transistors*, IEEE J. Explor. Solid-State Comput. Devices Circuits **1**, 28 (2015).

Correct implementation of polarization constants in wurtzite materials and impact on III-nitrides

Cyrus E. Dreyer

*Materials Department, University of California, Santa Barbara, CA 93106-5050 and
Department of Physics and Astronomy, Rutgers University, Piscataway, NJ 08845-0849*

Anderson Janotti* and Chris G. Van de Walle

Materials Department, University of California, Santa Barbara, CA 93106-5050

David Vanderbilt

*Department of Physics and Astronomy, Rutgers University, Piscataway, NJ 08845-0849
(Dated: September 25, 2018)*

Supplemental Material

S1. POLARIZATION IN ZINCBLLENDE

There is an additional subtlety when calculating the formal polarization of the zincblende (ZB) structure that is related to the choice of unit cell. If the primitive unit cell is used for the calculation [with the origin chosen such that the Ga atom is at $(-1/8, -1/8, -1/8)$ and the N at $(1/8, 1/8, 1/8)$], then the result for III-nitrides will be what was determined in Ref. S1, Section III E. Specifically, the electronic part of the polarization vanishes, so the contribution simply comes from \mathbf{P}_{ion} of Eq. (2) of the main text:

$$\mathbf{P}_{\text{f}}^{\text{ZB}} = \frac{e\sqrt{2}a_{\text{WZ}}}{\Omega} \left(\frac{1}{4}, \frac{1}{4}, \frac{1}{4} \right), \quad (1)$$

where the a_{WZ} is the in plane lattice parameter of the wurzite (WZ) material (related to the ZB lattice constant by $\sqrt{2}$). The magnitude in the [111] direction is therefore $\sqrt{3}ea_{\text{WZ}}/2\sqrt{2}\Omega = e\sqrt{3}/2a_{\text{WZ}}^2$ [since the volume of the ZB primitive cell is $\Omega = (\sqrt{2}a_{\text{WZ}})^3/4$]. Though choosing a different origin of the cell may change the value by quanta of polarization, there are no lattice vectors \mathbf{R} of the primitive ZB cell [$\sqrt{2}a_{\text{WZ}}(1/2, 1/2, 0)$, $\sqrt{2}a_{\text{WZ}}(0, 1/2, 1/2)$ and $\sqrt{2}a_{\text{WZ}}(1/2, 0, 1/2)$] that will result in a quantum of polarization $e\mathbf{R}/\Omega$ that will take $\mathbf{P}_{\text{f}}^{\text{ZB}}$ to zero, and therefore ZB truly has a nonvanishing formal polarization. For the III-nitrides, we list the values of formal polarization for ZB along with WZ and the layered hexagonal (H) structure in Table I below.

We note that if a conventional eight-atom cubic unit cell is used, the results are misleading. The cubic cell volume is four times that of the primitive cell, $\Omega_c = 4\Omega$, and has four ‘‘dipoles’’ such as the one in Eq. (1); therefore, the magnitude of the polarization vector in the [111] direction is four times larger. Equation (1) now becomes:

$$\mathbf{P}_{\text{f}}^{\text{ZB}}(\text{cubic cell}) = \frac{e\sqrt{2}a_{\text{WZ}}}{\Omega_c} (1, 1, 1). \quad (2)$$

However, $\sqrt{2}a_{\text{WZ}}(1, 1, 1)$ is now given by the sum of lattice vectors of the *cubic cell* [$\sqrt{2}a_{\text{WZ}}(1, 0, 0)$, $\sqrt{2}a_{\text{WZ}}(0, 1, 0)$, and $\sqrt{2}a_{\text{WZ}}(0, 0, 1)$]; therefore it appears that $\mathbf{P}_{\text{f}}^{\text{ZB}}(\text{cubic cell})$ vanishes modulo a quantum of polarization. The calculation

TABLE I. Calculated formal polarizations, in units of C/m², of wurtzite (WZ), zincblende (ZB) and layered hexagonal (H) GaN, AlN, and InN, all at the relaxed WZ in-plane lattice constant.

	$P_{\text{f}}^{(\text{WZ})}$	$P_{\text{f}}^{(\text{ZB})}$	$P_{\text{f}}^{(\text{H})}$
GaN	1.31	1.35	0
AlN	1.35	1.44	0
InN	1.03	1.07	0

* Current address: Materials Science and Engineering, University of Delaware, Newark, Delaware 19716-1501, USA

using the primitive cell is the rigorous result, as it is the smallest possible unit cell. For conventional unit cells of larger size, the quantum of polarization becomes smaller compared to the magnitude of the polarization vector, and the true values for the formal polarization cannot be ascertained.

S2. STRUCTURAL PARAMETERS AND BAND GAPS CALCULATED WITH THE HSE HYBRID FUNCTIONAL

TABLE II. Parameters for the III-nitrides calculated with HSE. Experimental data are listed for comparison.

	Property	HSE (this work)	Experiment ^a
GaN	a (Å)	3.205	3.189
	c (Å)	5.200	5.185
	u	0.377	0.377 ^b
	E_g (eV)	3.496	3.4-3.5
AlN	a (Å)	3.099	3.112
	c (Å)	4.959	4.982
	u	0.382	0.382 ^b
	E_g (eV)	6.044	6.1-6.3
InN	a (Å)	3.587	3.545
	c (Å)	5.762	5.703
	u	0.380	–
	E_g (eV)	0.646	0.6-0.8

^a From Ref. S2 unless otherwise specified.

^b From Ref. S3.

S3. EXPERIMENTAL DETERMINATION OF POLARIZATION FROM THE LITERATURE

The experimental data points in Fig. 2 of the main text were taken from various literature studies that were intended to determine the polarization constants in the InGaN/GaN or AlGaIn/GaN systems. We list these references in Table IV, V, VI, and III along with the reported values. Whether the actual measurement was bound charges at an interface or the field in a quantum well, we have converted the reported values to a polarization sheet charge for the purposes of Fig. 2 using the procedure outlined in Sec. V of the main text.

TABLE III. Experimental data for GaN/InGaIn/GaN quantum wells from optical (if not specified), holography, and CV measurements. In the cases where fields are reported in the reference, the bound charge is determined from the model described in the main text, Sec. V.

Reference	InGaIn content	Field (10^5 V/cm)	Bound charge ($10^{12}e^-/\text{cm}^2$)
S4	0.08	6.0	3.1
S5	0.10	13.6	7.2
S6	0.15	21.0	11.5
S7	0.12, 0.22	15.0, 29.0	8.1, 16.5
S8	0.10	3.5	1.9
S9	0.18, 0.15, 0.20	24.5, 27.0, 22.0	13.6, 14.8, 12.4
S10, S11, S12	0.07, 0.08, 0.08, 0.08, 0.08, 0.08, 0.09, 0.09, 0.09, 0.09, 0.09	10.5, 11.4, 11.1, 11.1, 12.6, 12.3, 12.9, 13.4, 13.7, 14.0, 14.0	5.5, 6.0, 5.8, 5.8, 6.6, 6.5, 6.8, 7.1, 7.2, 7.4, 7.4
S13	0.07	9.3	4.8
S14	0.15	13.4	7.33
S15	0.08	11.0	5.76
S16	0.09	19.0	10.0
S17	0.11		2.9
S18	0.20	31.0	17.5
S19	0.11	3.0	1.6
S20	0.10	9.0	4.8
S21	0.14, 0.14, 0.14	18.1, 21.2, 20.4	9.8, 11.5, 11.1
S22	0.16	12.0	6.6
S23	0.23	18.0	10.3
S23 (holography)	0.18	22	12.2
S24 (holography)	0.52	40.0	26.8
S25 (holography)	0.52	32.0	21.4
S26 (CV)	0.08		4.1
S27 (CV)	0.05, 0.09		1.8, 4.4

TABLE IV. Experimental data for GaN/AlGaN interfaces from Hall-effect measurements.

Reference	AlGaN content	Bound charge ($10^{12}e^-/\text{cm}^2$)
S28	0.09, 0.13, 0.17, 0.26, 0.31, 0.13, 0.18, 0.22, 0.22, 0.26, 0.29, 0.29, 0.31	3.9, 4.9, 8.7, 13.8, 15.0, 6.8, 7.2, 8.2, 11.0, 10.2, 10.1, 13.4, 13.5
S29	0.20, 0.20, 0.30, 0.35, 0.40, 0.40, 0.40, 0.40, 0.40, 0.37	9.8, 15.1, 19.1, 23.6, 28.5, 25.4, 24.1, 22.0, 19.7, 20.1
S30	0.33, 0.34, 0.38	13.2, 9.0, 10.5
S31	0.15	6.0
S32	0.15	7.9
S33	0.3 0	16.0
S34	0.05, 0.15	2.3, 6.7
S35	0.02, 0.06, 0.09, 0.14, 0.02, 0.05, 0.13, 0.15, 0.19, 0.24, 0.29	1.1, 2.1, 3.0, 3.3, 1.2, 1.6, 4.4, 4.6, 5.6, 6.5, 8.0
S36	0.12, 0.14, 0.14, 0.17, 0.17, 0.20, 0.23, 0.24, 0.26, 0.30, 0.31, 0.34, 0.36, 0.37	3.5, 4.6, 4.3, 5.6, 5.6, 6.5, 7.9, 8.8, 9.1, 10.7, 11.6, 12.3, 12.6, 14.0
S37	0.23	11.0
S38	0.16	7.3
S39	0.10, 0.13, 0.18	2.8, 4.1, 6.2
S40	0.10, 0.15, 0.20	4.1, 6.3, 8.7
S41	0.13, 0.23, 0.26, 0.36	7.3, 9.5, 11.0, 15.2
S42	0.22, 0.26, 0.32, 0.36	7.3, 9.0, 11.3, 12.0
S43	1.0	34
S44	0.20	13
S45	0.05, 0.15, 0.15, 0.15, 0.25, 0.35	3.0, 8.0, 7.5, 5.9, 9.9, 18.0
S46	0.23	9.8
S47	0.06, 0.10, 0.26, 0.33	1.0, 1.9, 1.4, 1.8
S48	0.72	35
S49	0.21, 0.21, 0.27, 0.33, 0.33, 0.40, 0.40, 0.49, 0.48	9.2, 10.1, 11.0, 11.5, 11.2, 12.9, 13.3, 16.9, 16.4
S50	0.15, 0.19, 0.18, 0.19, 0.20, 0.20, 0.23, 0.22, 0.26, 0.27, 0.26, 0.31, 0.31, 0.32, 0.32, 0.34, 0.35, 0.37, 0.37, 0.36, 0.43, 0.44, 0.46	0.7, 1.1, 1.4, 2.8, 3.0, 6.9, 6.4, 4.8, 11.2, 11.0, 8.7, 12.2, 13.0, 14.1, 9.8, 11.0, 9.6, 10.1, 11.4, 14.7, 13.6, 14.0, 14.3
S51	0.26	25

TABLE V. Experimental data for AlGaIn/GaN/AlGaIn quantum wells from optical and holography measurements. In the cases where fields are reported in the reference, the bound charge is determined from the model described in the main text, Sec. V.

Reference	AlGaIn content	Field (10^5 V/cm)	Bound charge ($10^{12}e^-/\text{cm}^2$)
S52	0.08, 0.08, 0.13, 0.17, 0.13, 0.17, 0.27, 0.27		3.8, 3.0, 5.6, 7.2, 7.4, 9.4, 14.2, 10.9
S53	0.15		2.0
S54	0.50	42.7	21.2
S55	0.20, 0.20	12.8, 8.3	6.4, 4.1
S55 (Holography)	0.20, 0.20, 0.20	12.8, 8.4, 6.9	6.4, 4.2, 3.4
S56	0.24	15.0	7.5
S57	0.17	8.3	4.1
S58	0.65	20	9.94
S59, S60	0.07	4.8	2.4
S61	0.14	5.1	2.5
S62	0.18, 0.11, 0.15	10.2, 9.3, 3.8	5.1, 4.6, 1.9
S63	0.18	12.3	6.1
S64	0.20, 0.50, 0.65, 0.80	11.9, 29.5, 33.9, 49.2	5.9, 14.6, 16.8, 24.5
S65	0.15	3.5	1.74
S57	0.11	4.5	2.24
S66	0.24, 0.18, 0.18, 0.15, 0.07, 0.18, 0.17, 0.16, 0.16	13.0, 13.0, 13.2, 9.0, 4.1, 13.3, 10.0, 10.0, 10.2	
S67	0.07, 0.15, 0.17, 0.18, 0.24, 0.18, 0.16, 0.16, 0.17	5.3, 11.7, 17.2, 16.9, 19.5, 13.8, 10.6, 10.2, 10.1	2.6, 5.8, 8.5, 8.4, 9.7, 6.9, 5.3, 5.1, 5.0
S68	0.15	14	7.0
S46	0.23		10.2
S47	0.06, 0.10, 0.26, 0.33	3.4, 3.1, 3.8, 3.4	1.7, 1.5, 1.9, 1.7
S69	0.31		11.0
S70			
S71	0.19	2.5	7.4

TABLE VI. Experimental data for GaN/AlGaIn interfaces from CV measurements.

Reference	AlGaIn content	Bound charge ($10^{12}e^-/\text{cm}^2$)
S72	0.22	1.3
S73	0.15	3.8
S50	0.33	10, 12
S74	0.09, 0.13, 0.17, 0.26, 0.31	3.8, 4.9, 8.7, 13.6, 15.0
S75	0.05, 0.12, 0.16	2.3, 6.8, 6.9
S26	0.13	7.1
S35	0.02, 0.06, 0.09, 0.14	0.9, 1.8, 2.0, 3.1
S51	0.26	7.0

S4. BOUND CHARGES AT NITRIDE INTERFACES

Here we present the specific equations used to generate Fig. 2 in the main text. As in the main text, we assume a coherent c plane interface of GaN and the alloy (InGa $_x$ N or AlGa $_x$ N), with the alloy layer under biaxial stress. The current practice in the field (black dashed curve in Fig. 2 of the main text) is to use the effective spontaneous (SP) polarization constants with respect to the zincblende (ZB) reference, without the correction term [$\Delta P_{\text{corr}}^{\text{ref}}$ introduced in Eq. (11) of the main text], and the proper piezoelectric (PZ) constants. (These values are usually taken from Ref. S76.) The resulting equation for Al $_x$ Ga $_{1-x}$ N/GaN is

$$\begin{aligned} \sigma_{\text{b}}^{(\text{ZB ref}),\text{prop}}(x) = & \Delta \tilde{P}_{\text{SP}}^{\text{int},(\text{ZB ref})} x - 2 \frac{(a_{\text{AlN}} - a_{\text{GaN}})x}{a_{\text{AlN}}x + a_{\text{GaN}}(1-x)} \left\{ e_{31}^{\text{AlN},\text{prop}} x + e_{31}^{\text{GaN},\text{prop}}(1-x) \right. \\ & \left. - [e_{33}^{\text{AlN},\text{prop}} x + e_{33}^{\text{GaN},\text{prop}}(1-x)] \frac{C_{13}^{\text{AlN}} x + C_{13}^{\text{GaN}}(1-x)}{C_{33}^{\text{AlN}} x + C_{33}^{\text{GaN}}(1-x)} \right\}, \end{aligned} \quad (3)$$

where $\Delta \tilde{P}_{\text{SP}}^{\text{int},(\text{ZB ref})}$ is

$$\Delta \tilde{P}_{\text{SP}}^{\text{int},(\text{ZB ref})} = P_{\text{eff}}^{\text{GaN},(\text{ZB ref})} - P_{\text{eff}}^{\text{AlN},(\text{ZB ref})}. \quad (4)$$

An identical set of equations are used for In $_x$ Ga $_{1-x}$ N/GaN, with InN instead of AlN.

The red solid curve in Fig. 2 corresponds to using the H ref (or ZB with the correction term) and the improper PZ constants:

$$\begin{aligned} \sigma_{\text{b}}^{(\text{H ref}),\text{imp}}(x) = & \Delta \tilde{P}_{\text{SP}}^{\text{int},(\text{H ref})} x - 2 \frac{(a_{\text{AlN}} - a_{\text{GaN}})x}{a_{\text{AlN}}x + a_{\text{GaN}}(1-x)} \left\{ \left(e_{31}^{\text{AlN},\text{prop}} - P_{\text{eff}}^{\text{AlN},(\text{H ref})} \right) x \right. \\ & \left. + \left(e_{31}^{\text{GaN},\text{prop}} - P_{\text{eff}}^{\text{GaN},(\text{H ref})} \right) (1-x) - [e_{33}^{\text{AlN},\text{prop}} x + e_{33}^{\text{GaN},\text{prop}}(1-x)] \frac{C_{13}^{\text{AlN}} x + C_{13}^{\text{GaN}}(1-x)}{C_{33}^{\text{AlN}} x + C_{33}^{\text{GaN}}(1-x)} \right\} \\ = & (\Delta \tilde{P}_{\text{SP}}^{\text{int},(\text{ZB ref})} + \Delta P_{\text{corr}}^{(\text{ZB ref})}) x - 2 \frac{(a_{\text{AlN}} - a_{\text{GaN}})x}{a_{\text{AlN}}x + a_{\text{GaN}}(1-x)} \left\{ \left(e_{31}^{\text{AlN},\text{prop}} - P_{\text{eff}}^{\text{AlN},(\text{H ref})} \right) x \right. \\ & \left. + \left(e_{31}^{\text{GaN},\text{prop}} - P_{\text{eff}}^{\text{GaN},(\text{H ref})} \right) (1-x) - [e_{33}^{\text{AlN},\text{prop}} x + e_{33}^{\text{GaN},\text{prop}}(1-x)] \frac{C_{13}^{\text{AlN}} x + C_{13}^{\text{GaN}}(1-x)}{C_{33}^{\text{AlN}} x + C_{33}^{\text{GaN}}(1-x)} \right\}, \end{aligned} \quad (5)$$

where

$$\Delta P_{\text{corr}}^{(\text{ZB ref})} = \frac{e\sqrt{3}}{2} \left(\frac{1}{(a_{\text{GaN}})^2} - \frac{1}{(a_{\text{AlN}})^2} \right), \quad (6)$$

and similarly for InGa $_x$ N/GaN.

S5. DIFFERENCE BETWEEN IMPLEMENTATIONS

The difference between the current practice in the field (ZB reference, no correction term, proper PZ) and our revised implementation (H reference, improper PZ constants) can be determined by taking the difference of Eq. (3) and Eq. (5). For the case of AlGa_N/Ga_N:

$$\begin{aligned}
\sigma_b^{(\text{H ref}), \text{imp}}(x) - \sigma_b^{(\text{ZB ref}), \text{prop}}(x) &= x \left[\Delta \tilde{P}_{\text{SP}}^{\text{int}, (\text{H ref})} - \Delta \tilde{P}_{\text{SP}}^{\text{int}, (\text{ZB ref})} \right] \\
&\quad - 2 \frac{(a_{\text{AlN}} - a_{\text{GaN}})x}{a_{\text{AlN}}x + a_{\text{GaN}}(1-x)} \left[-P_{\text{eff}}^{\text{AlN}, (\text{H ref})}(x) - P_{\text{eff}}^{\text{GaN}, (\text{H ref})}(1-x) \right] \\
&= x \left[\left(\Delta \tilde{P}_{\text{SP}}^{\text{int}, (\text{ZB ref})} + \Delta P_{\text{corr}}^{(\text{ZB ref})} \right) - \Delta \tilde{P}_{\text{SP}}^{\text{int}, (\text{ZB ref})} \right] \\
&\quad + 2 \frac{(a_{\text{AlN}} - a_{\text{GaN}})x}{a_{\text{AlN}}x + a_{\text{GaN}}(1-x)} \left[P_{\text{eff}}^{\text{AlN}, (\text{H ref})}(x) + P_{\text{eff}}^{\text{GaN}, (\text{H ref})}(1-x) \right] \\
&= x \Delta P_{\text{corr}}^{(\text{ZB ref})} + 2 \frac{(a_{\text{AlN}} - a_{\text{GaN}})x}{a_{\text{AlN}}x + a_{\text{GaN}}(1-x)} \left[P_{\text{eff}}^{\text{AlN}, (\text{H ref})}(x) + P_{\text{eff}}^{\text{GaN}, (\text{H ref})}(1-x) \right] \\
&= x \Delta P_{\text{corr}}^{(\text{ZB ref})} + 2\varepsilon_1(x) P_{\text{eff}}^{\text{AlGaN}, (\text{H ref})}(x).
\end{aligned} \tag{7}$$

We can gain some more insight by linearizing the first term in Eq. (7):

$$\begin{aligned}
x \Delta P_{\text{corr}}^{(\text{ZB ref})} &= x \frac{e\sqrt{3}}{2} \left(\frac{1}{(a_{\text{GaN}})^2} - \frac{1}{(a_{\text{AlN}})^2} \right) \\
&= x \frac{e\sqrt{3}}{2} \frac{1}{(a_{\text{GaN}})^2} \left(1 - \frac{(a_{\text{GaN}})^2}{(a_{\text{AlN}})^2} \right) \\
&= x P_f^{\text{GaN}, \text{ZB}} \left(1 - \frac{(a_{\text{GaN}})^2}{(a_{\text{AlN}})^2} \right) \\
&\simeq 2x P_f^{\text{GaN}, \text{ZB}} \left(1 - \frac{a_{\text{GaN}}}{a_{\text{AlN}}} \right) \\
&= -2P_f^{\text{GaN}, \text{ZB}} \left(x \frac{a_{\text{GaN}} - a_{\text{AlN}}}{a_{\text{AlN}}} \right) \\
&\simeq -2P_f^{\text{GaN}, \text{ZB}} \varepsilon_1(x)
\end{aligned} \tag{8}$$

So we see that the difference in implementations is

$$\begin{aligned}
\sigma_b^{(\text{H ref}), \text{imp}}(x) - \sigma_b^{(\text{ZB ref}), \text{prop}}(x) &\simeq 2\varepsilon_1(x) \left[P_{\text{eff}}^{\text{AlGaN}, (\text{H ref})}(x) - P_f^{\text{GaN}, \text{ZB}} \right] \\
&= 2\varepsilon_1(x) \left[x P_f^{\text{AlN}, \text{WZ}} + (1-x) P_f^{\text{GaN}, \text{WZ}} - P_f^{\text{GaN}, \text{ZB}} \right] \\
&= 2\varepsilon_1(x) \left[x \left(P_f^{\text{AlN}, \text{WZ}} - P_f^{\text{GaN}, \text{WZ}} \right) + \left(P_f^{\text{GaN}, \text{WZ}} - P_f^{\text{GaN}, \text{ZB}} \right) \right] \\
&= 2\varepsilon_1(x) \left[x \left(P_f^{\text{AlN}, \text{WZ}} - P_f^{\text{GaN}, \text{WZ}} \right) + P_{\text{eff}}^{\text{GaN}, (\text{ZB ref})} \right]
\end{aligned} \tag{9}$$

Therefore, the difference is small for small strains, and/or when there is a large cancellation of the terms in the square brackets. We see from Table I of the main text that $P_f^{\text{AlN}, \text{WZ}} - P_f^{\text{GaN}, \text{WZ}} = 0.039 \text{ C/m}^2 \sim -P_{\text{eff}}^{\text{GaN}, (\text{ZB ref})}$, hence the close agreement with between the black dashed and red solid curves in Fig. 2(b) of the main text (along with the relatively small magnitude of the strain). For the case of InGa_N, $P_f^{\text{InN}, \text{WZ}} - P_f^{\text{GaN}, \text{WZ}} = -0.286 \text{ C/m}^2$ which is the same sign as $P_{\text{eff}}^{\text{GaN}, (\text{ZB ref})}$, hence the larger discrepancy between the black dashed and red solid curves in Fig. 2(a) of the main text (also combined with a larger strain between InN and GaN).

[S1] D. Vanderbilt and R. D. King-Smith, “Electric polarization as a bulk quantity and its relation to surface charge,” Phys. Rev. B **48**, 4442 (1993).

- [S2] I. Vurgaftman and J. R. Meyer, “Band parameters for nitrogen-containing semiconductors,” *J. Appl. Phys.* **94**, 3675 (2003).
- [S3] H. Schulz and K.H. Thiemann, “Crystal structure refinement of AlN and GaN,” *Solid State Commun.* **23**, 815 (1977).
- [S4] M. E. Aumer, S. F. LeBoeuf, B. F. Moody, and S. M. Bedair, “Strain-induced piezoelectric field effects on light emission energy and intensity from AlInGaN/InGaN quantum wells,” *Appl. Phys. Lett.* **79**, 3803 (2001).
- [S5] Q. Li, S. J. Xu, M. H. Xie, S. Y. Tong, X. H. Zhang, W. Liu, and S. J. Chua, “Strong screening effect of photo-generated carriers on piezoelectric field in $\text{In}_{0.13}\text{Ga}_{0.87}\text{N}/\text{In}_{0.03}\text{Ga}_{0.97}\text{N}$ quantum wells,” *Jpn. J. Appl. Phys.* **41**, L1093 (2002).
- [S6] Y. D. Jho, J. S. Yahng, E. Oh, and D. S. Kim, “Measurement of piezoelectric field and tunneling times in strongly biased InGaN/GaN quantum wells,” *Appl. Phys. Lett.* **79**, 1130 (2001).
- [S7] A. Hangleiter, F. Hitzel, S. Lahmann, and U. Rossow, “Composition dependence of polarization fields in GaInN/GaN quantum wells,” *Appl. Phys. Lett.* **83**, 1169 (2003).
- [S8] S. F. Chichibu, A. C. Abare, M. S. Minsky, S. Keller, S. B. Fleischer, J. E. Bowers, E. Hu, U. K. Mishra, L. A. Coldren, S. P. DenBaars, and T. Sota, “Effective band gap inhomogeneity and piezoelectric field in InGaN/GaN multiquantum well structures,” *Appl. Phys. Lett.* **73**, 2006 (1998).
- [S9] P. Lefebvre, A. Morel, M. Gallart, T. Taliercio, J. Allgre, B. Gil, H. Mathieu, B. Damilano, N. Grandjean, and J. Massies, “High internal electric field in a graded-width InGaN/GaN quantum well: Accurate determination by time-resolved photoluminescence spectroscopy,” *Appl. Phys. Lett.* **78**, 1252 (2001).
- [S10] P. Kiesel, F. Renner, M. Kneissl, C. G. Van de Walle, G. H. Döhler, and N. M. Johnson, “Electroabsorption Spectroscopy – Direct Determination of the Strong Piezoelectric Field in InGaN/GaN Heterostructure Diodes,” *Phys. Stat. Sol. (a)* **188**, 131 (2001).
- [S11] P. Kiesel, F. Renner, M. Kneissl, C. G. Van de Walle, G. H. Döhler, and N. M. Johnson, “Quantitative Analysis of Absorption and Field-Induced Absorption Changes in InGaN/GaN Quantum Wells,” *Phys. Stat. Sol. (b)* **234**, 742–745 (2002).
- [S12] F. Renner, P. Kiesel, G. H. Döhler, M. Kneissl, C. G. Van de Walle, and N. M. Johnson, “Quantitative analysis of the polarization fields and absorption changes in InGaN/GaN quantum wells with electroabsorption spectroscopy,” *Appl. Phys. Lett.* **81**, 490 (2002).
- [S13] R. J. Kaplar, S. R. Kurtz, D. D. Koleske, and A. J. Fischer, “Electroreflectance studies of Stark shifts and polarization-induced electric fields in InGaN/GaN single quantum wells,” *J. Appl. Phys.* **95**, 4905 (2004).
- [S14] S.-M. Kim, H. S. Oh, J. H. Baek, K.-H. Lee, G. Y. Jung, J.-H. Song, H.-J. Kim, B.-J. Ahn, D. Yanqun, and J.-H. Song, “Effects of patterned sapphire substrates on piezoelectric field in blue-emitting InGaN multiple quantum wells,” *IEEE Electr. Device Lett.* **31**, 842 (2010).
- [S15] G. Franssen, P. Perlin, and T. Suski, “Photocurrent spectroscopy as a tool for determining piezoelectric fields in $\text{In}_x\text{Ga}_{1-x}\text{N}/\text{GaN}$ multiple quantum well light emitting diodes,” *Phys. Rev. B* **69**, 045310 (2004).
- [S16] I. H. Brown, I. A. Pope, P. M. Smowton, P. Blood, J. D. Thomson, W. W. Chow, D. P. Bour, and M. Kneissl, “Determination of the piezoelectric field in InGaN quantum wells,” *Appl. Phys. Lett.* **86**, 131108 (2005).
- [S17] M. Thomsen, H. Jönen, U. Rossow, and A. Hangleiter, “Effects of spontaneous polarization on GaInN/GaN quantum well structures,” *J. Appl. Phys.* **109**, 123710 (2011).
- [S18] D. Turchinovich, P. Uhd Jepsen, B. Monozon, M. Koch, S. Lahmann, U. Rossow, and A. Hangleiter, “Ultrafast polarization dynamics in biased quantum wells under strong femtosecond optical excitation,” *Phys. Rev. B* **68**, 241307 (2003).
- [S19] O. Gfrörer, C. Gemmer, J. Off, J. S. Im, F. Scholz, and A. Hangleiter, “Direct Observation of Pyroelectric Fields in InGaN/GaN and AlGaIn/GaN Heterostructures,” *Phys. Stat. Sol. (b)* **216**, 405–408 (1999).
- [S20] E. Berkowicz, D. Gershoni, G. Bahir, A. C. Abare, S. P. DenBaars, and L. A. Coldren, “Optical spectroscopy of InGaN/GaN quantum wells,” *Phys. Stat. Sol. (b)* **216**, 291–300 (1999).
- [S21] S. I. Park, J. I. Lee, and D. H. Jang, “Measurement of Internal Electric Field in GaN-Based Light-Emitting Diodes,” *IEEE J. Quantum Elect.* **48**, 500 (2012).
- [S22] T. Takeuchi, C. Wetzels, S. Yamaguchi, H. Sakai, H. Amano, I. Akasaki, Y. Kaneko, S. Nakagawa, Y. Yamaoka, and N. Yamada, “Determination of piezoelectric fields in strained GaInN quantum wells using the quantum-confined Stark effect,” *Appl. Phys. Lett.* **73**, 1691 (1998).
- [S23] C. Y. Lai, T. M. Hsu, W.-H. Chang, K.-U. Tseng, C.-M. Lee, C.-C. Chuo, and J.-I. Chyi, “Direct measurement of piezoelectric field in $\text{In}_{0.23}\text{Ga}_{0.77}\text{N}/\text{GaN}$ multiple quantum wells by electrotransmission spectroscopy,” *J. Appl. Phys.* **91**, 531 (2002).
- [S24] D. Cherns, J. Barnard, and F. A. Ponce, “Measurement of the piezoelectric field across strained InGaN/GaN layers by electron holography,” *Solid State Commun.* **111**, 281 (1999).
- [S25] J. S. Barnard and D. Cherns, “Direct observation of piezoelectric fields in GaN/ InGaN/GaN strained quantum wells,” *J. Electron Microsc.* **49**, 281 (2000).
- [S26] L. Jia, E. T. Yu, D. Keogh, P. M. Asbeck, P. Miraglia, A. Roskowski, and R. F. Davis, “Polarization charges and polarization-induced barriers in $\text{Al}_x\text{Ga}_{1-x}\text{N}/\text{GaN}$ and $\text{In}_y\text{Ga}_{1-y}\text{N}/\text{GaN}$ heterostructures,” *Appl. Phys. Lett.* **79**, 2916 (2001).
- [S27] X. H. Zhang, W. Liu, and S. J. Chua, “Optical transitions in InGaN/GaN quantum wells: effects of the piezoelectric field,” *J. Cryst. Growth* **268**, 521 (2004).
- [S28] Y. Zhang, I. P. Smorchkova, C. R. Elsass, S. Keller, J. P. Ibbetson, S. Denbaars, U. K. Mishra, and J. Singh, “Charge control and mobility in AlGaIn/GaN transistors: Experimental and theoretical studies,” *J. of Appl. Phys.* **87**, 7981 (2000).
- [S29] S. K. Davidsson, M. Gurusinge, T. G. Andersson, and H. Zirath, “The influence of composition and unintentional doping on the two-dimensional electron gas density in AlGaIn/GaN heterostructures,” *J. of Electron. Mater.* **33**, 440 (2004).

- [S30] G. Martínez-Criado, A. Cros, A. Cantarero, O. Ambacher, C. R. Miskys, R. Dimitrov, M. Stutzmann, J. Smart, and J. R. Shealy, “Residual strain effects on the two-dimensional electron gas concentration of AlGa_xN/GaN heterostructures,” *J. Appl. Phys.* **90**, 4735 (2001).
- [S31] S. C. Binari, J. M. Redwing, G. Kelner, and W. Kruppa, “AlGa_xN/GaN HEMTs grown on SiC substrates,” *Electron. Lett.* **33**, 242 (1997).
- [S32] Y.-F. Wu, B. P. Keller, S. Keller, D. Kapolnek, P. Kozodoy, S. P. Denbaars, and U. K. Mishra, “Very high breakdown voltage and large transconductance realized on GaN heterojunction field effect transistors,” *Appl. Phys. Lett.* **69**, 1438 (1996).
- [S33] C. Nguyen, N. X. Nguyen, M. Le, and D. E. Grider, “High performance GaN/AlGa_xN MODFETs grown by RF-assisted MBE,” *Electron. Lett.* **34**, 309 (1998).
- [S34] L. W. Wong, S. J. Cai, R. Li, K. Wang, H. W. Jiang, and M. Chen, “Magnetotransport study on the two-dimensional electron gas in AlGa_xN/GaN heterostructures,” *Appl. Phys. Lett.* **73**, 1391 (1998).
- [S35] K. Köhler, S. Müller, P. Waltereit, W. Pletschen, V. Polyakov, T. Lim, L. Kirste, H. P. Menner, P. Brückner, O. Ambacher, C. Buchheim, and R. Goldhahn, “Electrical properties of Al_xGa_{1-x}N/GaN heterostructures with low Al content,” *J. Appl. Phys.* **109**, 053705 (2011).
- [S36] K. Köhler, S. Müller, Patrick Waltereit, L. Kirste, H. P. Menner, W. Bronner, and Rüdiger Quay, “Growth and electrical properties applications and materials science of Al_xGa_{1-x}N/GaN heterostructures with different Al-content,” *Phys. Stat. Sol. (a)* **206**, 2652 (2009).
- [S37] A. Naka^jima, Y. Sumida, M. H. Dhyani, H. Kawai, and E. M. S. Narayanan, “High Density Two-Dimensional Hole Gas Induced by Negative Polarization at GaN/AlGa_xN Heterointerface,” *Appl. Phys. Express* **3**, 121004 (2010).
- [S38] J. Burm, W. J. Schaff, L. F. Eastman, H. Amano, and I. Akasaki, “75 Å GaN channel modulation doped field effect transistors,” *Appl. Phys. Lett.* **68**, 2849 (1996).
- [S39] T. Wang, Y. Ohno, M. Lachab, D. Nakagawa, T. Shirahama, S. Sakai, and H. Ohno, “Electron mobility exceeding 10⁴ cm²/V s in an AlGa_xN/GaN heterostructure grown on a sapphire substrate,” *Appl. Phys. Lett.* **74**, 3531 (1999).
- [S40] Y. Liu, M. Z. Kausar, D. D. Schroepfer, P. P. Ruden, J. Xie, Y. T. Moon, N. Onojima, H. Morkoç, K.-A. Son, and M. I. Nathan, “Effect of hydrostatic pressure on the current-voltage characteristics of GaN/AlGa_xN/GaN heterostructure devices,” *J. Appl. Phys.* **99**, 113706 (2006).
- [S41] G. J. Ding, L. W. Guo, Z. G. Xing, Y. Chen, P. Q. Xu, H. Q. Jia, J. M. Zhou, and H. Chen, “Characterization of different-Al-content AlGa_xN/GaN heterostructures on sapphire,” *Sci. China Phys. Mech. Astron.* **53**, 49– (2010).
- [S42] W. S. Chen, S. J. Chang, Y. K. Su, R. L. Wang, C. H. Kuo, and S. C. Shei, “Al_xGa_{1-x}N/GaN heterostructure field effect transistors with various Al mole fractions in AlGa_xN barrier,” *J. Cryst. Growth* **275**, 398 (2005).
- [S43] K. Jeganathan, T. Ide, M. Shimizu, and H. Okumura, “Two-dimensional electron gases induced by polarization charges in AlN/GaN heterostructure grown by plasma-assisted molecular-beam epitaxy,” *J. Appl. Phys.* **94**, 3260 (2003).
- [S44] R. Gaska, A. Osinsky, J. W. Yang, and M. S. Shur, “Self-Heating in High-Power AlGa_xN-GaN HFETs,” *IEEE Electr. Device Lett.* **19**, 89 (1998).
- [S45] P. M. Asbeck, E. T. Yu, S. S. Lau, G. J. Sullivan, J. Van Hove, and J. Redwing, “Piezoelectric charge densities in AlGa_xN/GaN HFETs,” *Electron. Lett.* **33**, 1230 (1997).
- [S46] D.-P. Wang, C.-C. Wu, and C.-C. Wu, “Determination of polarization charge density on interface of AlGa_xN/GaN heterostructure by electroreflectance,” *Appl. Phys. Lett.* **89**, 161903 (2006).
- [S47] A. T. Winzer, R. Goldhahn, C. Buchheim, O. Ambacher, A. Link, M. Stutzmann, Y. Smorchkova, U. K. Mishra, and J. S. Speck, “Photorefectance studies of N- and Ga-face AlGa_xN/GaN heterostructures confining a polarization induced 2DEG,” *Phys. Stat. Sol. (b)* **240**, 380 (2003).
- [S48] G. Li, Y. Cao, H. G. Xing, and D. Jena, “High mobility two-dimensional electron gases in nitride heterostructures with high Al composition AlGa_xN alloy barriers,” *Appl. Phys. Lett.* **97**, 222110 (2010).
- [S49] S. Arulkumaran, T. Egawa, H. Ishikawa, and T. Jimbo, “Characterization of different-Al-content Al_xGa_{1-x}N/GaN heterostructures and high-electron-mobility transistors on sapphire,” *J. Vac. Sci. Technol. B* **21**, 888 (2003).
- [S50] O. Ambacher, B. Foutz, J. Smart, J. R. Shealy, N. G. Weimann, K. Chu, M. Murphy, A. J. Sierakowski, W. J. Schaff, L. F. Eastman, R. Dimitrov, A. Mitchell, and M. Stutzmann, “Two dimensional electron gases induced by spontaneous and piezoelectric polarization in undoped and doped AlGa_xN/GaN heterostructures,” *J. Appl. Phys.* **87**, 334 (2000).
- [S51] G. Franssen, J. A. Plesiewicz, L. H. Dmowski, P. Prystawko, T. Suski, W. Krupczyński, R. Jachymek, P. Perlin, and M. Leszczyński, “Hydrostatic pressure dependence of polarization-induced interface charge in AlGa_xN/GaN heterostructures determined by means of capacitance-voltage characterization,” *J. Appl. Phys.* **100**, 113712 (2006).
- [S52] N. Grandjean, B. Damilano, S. Dalmasso, M. Leroux, M. Lagt, and J. Massies, “Built-in electric-field effects in wurtzite AlGa_xN/GaN quantum wells,” *J. Appl. Phys.* **86**, 3714 (1999).
- [S53] R. Cingolani, A. Botchkarev, H. Tang, H. Morkoç, G. Traetta, G. Coli, M. Lomascolo, A. Di Carlo, F. Della Sala, and P. Lugli, “Spontaneous polarization and piezoelectric field in GaN/Al_{0.15}Ga_{0.85}N quantum wells: Impact on the optical spectra,” *Phys. Rev. B* **61**, 2711 (2000).
- [S54] G. Chen, Z. L. Li, X. Q. Wang, C. C. Huang, X. Rong, L. W. Sang, F. J. Xu, N. Tang, Z. X. Qin, M. Sumiya, Y. H. Chen, W. K. Ge, and B. Shen, “Effect of polarization on intersubband transition in AlGa_xN/GaN multiple quantum wells,” *Appl. Phys. Lett.* **102**, 192109 (2013).
- [S55] C. McAleese, P. M. F. J. Costa, D. M. Graham, H. Xiu, J. S. Barnard, M. J. Kappers, P. Dawson, M. J. Godfrey, and C. J. Humphreys, “Electric fields in AlGa_xN/GaN quantum well structures,” *Phys. Stat. Sol. (b)* **243**, 1551 (2006).
- [S56] R. Langer, J. Simon, V. Ortiz, N. T. Pelekanos, A. Barski, R. André, and M. Godlewski, “Giant electric fields in unstrained GaN single quantum wells,” *Appl. Phys. Lett.* **74**, 3827 (1999).

- [S57] M. Leroux, N. Grandjean, M. Laißt, J. Massies, B. Gil, P. Lefebvre, and P. Bigenwald, “Quantum confined Stark effect due to built-in internal polarization fields in (Al,Ga)N/GaN quantum wells,” *Phys. Rev. B* **58**, R13371 (1998).
- [S58] N. Suzuki and N. Iizuka, “Effect of Polarization Field on Intersubband Transition in AlGaIn/GaN Quantum Wells,” *Jpn. J. Appl. Phys.* **38**, L363 (1999).
- [S59] M. Esmaeili, M. Gholami, H. Haratizadeh, B. Monemar, P. O. Holtz, S. Kamiyama, H. Amano, and I. Akasaki, “Experimental and theoretical investigations of optical properties of GaN/AlGaIn MQW nanostructures. Impact of built-in polarization fields,” *Opto-Electron. Rev.* **17**, 293 (2009).
- [S60] M. Esmaeili, M. Sabooni, H. Haratizadeh, P. P. Paskov, B. Monemar, P. O. Holz, S. Kamiyama, and M. Iwaya, “Optical properties of GaN/AlGaIn QW nanostructures with different well and barrier widths,” *J. Phys: Condens. Mat.* **19**, 356218 (2007).
- [S61] A. Pinos, S. Marcinkevičius, K. Liu, M. S. Shur, E. Kuokštis, G. Tamulaitis, R. Gaska, J. Yang, and W. Sun, “Screening dynamics of intrinsic electric field in AlGaIn quantum wells,” *Appl. Phys. Lett.* **92**, 061907 (2008).
- [S62] S. Marcinkevičius, A. Pinos, K. Liu, D. Veksler, M. S. Shur, J. Zhang, and R. Gaska, “Intrinsic electric fields in AlGaIn quantum wells,” *Appl. Phys. Lett.* **90**, 081914 (2007).
- [S63] E. Kuokstis, C. Q. Chen, M. E. Gaevski, W. H. Sun, J. W. Yang, G. Simin, M. Asif Khan, H. P. Maruska, D. W. Hill, M. C. Chou, J. J. Gallagher, and B. Chai, “Polarization effects in photoluminescence of *c*- and *m*-plane GaN/AlGaIn multiple quantum wells,” *Appl. Phys. Lett.* **81**, 4130 (2002).
- [S64] H. M. Ng, R. Harel, S. N. G. Chu, and A. Y. Cho, “The effect of built-in electric field in GaN/AlGaIn quantum wells with high AlN mole fraction,” *J. Electron. Mater.* **30**, 134 (2001).
- [S65] J. S. Im, H. Kollmer, J. Off, A. Sohmer, F. Scholz, and A. Hangleiter, “Reduction of oscillator strength due to piezoelectric fields in GaN/Al_xGa_{1-x}N quantum wells,” *Phys. Rev. B* **57**, R9435 (1998).
- [S66] J. Simon, R. Langer, A. Barski, and N. Pelekanos, “Spontaneous polarization effects in GaN/Al_xGa_{1-x}N quantum wells,” *Phys. Rev. B* **61**, 7211–7214 (2000).
- [S67] J. Simon, R. Langer, A. Barski, M. Zervos, and N. T. Pelekanos, “Residual doping effects on the amplitude of polarization-induced electric fields in GaN/AlGaIn quantum wells,” *Phys. Stat. Sol. (a)* **188**, 867 (2001).
- [S68] O. Gfrörer, T. Schlüsener, V. Härle, F. Scholz, and A. Hangleiter, “Mechanisms of Strain Reduction in GaN and AlGaIn/GaN Epitaxial Layers,” *MRS Proc.* **449**, 429 (2011).
- [S69] A. T. Winzer, R. Goldhahn, G. Gobsch, A. Link, M. Eickhoff, U. Rossow, and A. Hangleiter, “Determination of the polarization discontinuity at the AlGaIn/GaN interface by electroreflectance spectroscopy,” *Appl. Phys. Lett.* **86**, 1–3 (2005).
- [S70] A. Drabińska, K. P. Korona, R. Božek, J. M. Baranowski, K. Pakul a, T. Tomaszewicz, and J. Gronkowski, “Investigation of 2D Electron Gas on AlGaIn/GaN Interface by Electroreflectance,” *Phys. Stat. Sol. (c)* **333**, 329 (2003).
- [S71] S. R. Kurtz, A. A. Allerman, D. D. Koleske, A. G. Baca, and R. D. Briggs, “Electronic properties of the AlGaIn/GaN heterostructure and two-dimensional electron gas observed by electroreflectance,” *J. Appl. Phys.* **95**, 1888 (2004).
- [S72] Y.-G. Zhou, B. Shen, T. Someya, H.-Q. Yu, J. Liu, H.-M. Zhou, R. Zhang, Y. Shi, Y.-D. Zheng, and Y. Arakawa, “Investigation of the polarization-induced charges in modulation-doped Al_xGa_{1-x}N/GaN heterostructures through capacitance-voltage profiling and simulation,” *Jpn. J. Appl. Phys.* **41**, 2531 (2002).
- [S73] E. T. Yu, G. J. Sullivan, P. M. Asbeck, C. D. Wang, D. Qiao, and S. S. Lau, “Measurement of piezoelectrically induced charge in GaN/AlGaIn heterostructure field-effect transistors,” *Appl. Phys. Lett.* **71**, 2794 (1997).
- [S74] I. P. Smorchkova, C. R. Elsass, J. P. Ibbetson, R. Vetury, B. Heying, P. Fini, E. Haus, S. P. DenBaars, J. S. Speck, and U. K. Mishra, “Polarization-induced charge and electron mobility in AlGaIn/GaN heterostructures grown by plasma-assisted molecular-beam epitaxy,” *J. Appl. Phys.* **86**, 4520 (1999).
- [S75] E. J. Miller, E. T. Yu, C. Poblenz, C. Elsass, and J. S. Speck, “Direct measurement of the polarization charge in AlGaIn/GaN heterostructures using capacitance-voltage carrier profiling,” *Appl. Phys. Lett.* **80**, 3551 (2002).
- [S76] F. Bernardini, V. Fiorentini, and D. Vanderbilt, “Spontaneous polarization and piezoelectric constants of III-V nitrides,” *Phys. Rev. B* **56**, R10024 (1997).